Restoring volcanic ocean island palaeotopography to uncover island-scale buried sector collapses

F.O. Marques, C.S. Catita, A. Hildenbrand, S.S. Victória

Restoring volcanic ocean island palaeotopography to uncover island-scale buried sector collapses

F.O. Marques*, C.S. Catita[1], A. Hildenbrand[2], S.S. Victória[3]

** Corresponding author, retired, no institutional affiliation, Portugal*

[1] Faculdade de Ciências e Instituto Dom Luiz, Universidade de Lisboa, 1749-016 Lisboa, Portugal

[2] Université Paris-Saclay, CNRS, GEOPS, Orsay, 91405, France

[3] Faculdade de Ciências e Tecnologia and Center for Local Development and Spatial Planning, Universidade de Cabo Verde, Praia, Santiago, Cabo Verde

Abstract

A volcanic edifice much larger than the current one must have existed in Santiago Island, Cape Verde, because the granular rocks and dyke-in-dyke complex representing magma chambers and deep feeders currently outcrop up to 700 m altitude. Therefore, we aim to find an explanation for the massive destruction of the original edifice. We developed a new tool for the quantitative reconstruction of ancient topographies in a volcanic ocean island to address this problem, because it allows us to estimate the shape and volume of volcanic rock removed at a certain time. The reconstruction of the topography of the basement complex at ca. 6 Ma ago, before the unconformable deposition of a submarine complex, shows a large eastward concave depression coincident with the asymmetric distribution of volcanic complexes east and west of

21 the eastward concave main divide of the island. This concave depression is here interpreted as
22 the scar of an island-scale, east-directed, sector collapse. Given the position of Santiago relative
23 to the nearby Maio Island, which could work as a buttress in the east, we conclude that the debris
24 generated by the inferred eastward collapse might have been diverted to the northeast. A west-
25 directed sector collapse can be recognised from the topography of the island and marine
26 geophysical data, which supports, by similarity, the sector collapse inferred for eastern Santiago.
27 This methodology could be replicated in many other oceanic islands worldwide where granular
28 rocks currently outcrop above sea level.

29

30 **Introduction**

31 Volcanic ocean islands evolve by interacting/alternating construction (volcanism) and
32 destruction (erosion in its different forms) episodes. When the volcanic edifice reaches a critical
33 mass, it becomes gravitationally unstable and eventually destabilises through spreading (slow)
34 and/or large-scale catastrophic flank collapses (fast). The remnants of the collapsed island,
35 especially the scar surface, are usually covered by a new phase of volcanic construction, which
36 may conceal significant parts of the collapsed island (e.g., Navarro and Coello, 1989; Day et al.,
37 1999; Hildenbrand et al., 2004; Quidelleur et al., 2006; Manconi et al., 2009; Boulesteix et al.,
38 2012; 2013; Maccaferri et al., 2017). In such a case, one must find a way of recovering the collapse-
39 related topography to analyse its main features. Otherwise, a great deal of critical information may
40 be lost.

41 Holcomb and Searle (1991) recognised that "… *seacliffs previously attributed to marine*
42 *erosion of many additional islands may instead be headwalls of still other landslides. These*

43 *landslides occur in a wide range of settings and probably represent only a small sample from a*
44 *large population*". This is what we kept in mind when we analysed Santiago's morphology, mostly
45 looking for large-scale embayments, present and past, in the Digital Elevation Model (DEM). Then
46 we compared Santiago's morphology with the geological map and the more recent geological data
47 to complete the picture. Lateral contacts between main geological units were especially
48 scrutinised, as they may witness strong geometric imbrication between successive construction
49 and destruction processes.

50 The reconstruction of the collapse-related topography is the main objective of this study,
51 with the ultimate goal of explaining what kind of erosion has destroyed a large volcanic edifice,
52 much larger than the current one, to the point of showing its deep core currently outcropping up to
53 700 m altitude. Our study further brings quantitative geomorphological constraints on the long-
54 term architectural evolution of volcanic islands, which may have significant societal implications,
55 e.g. regarding high-magnitude hazardous mass-wasting processes.

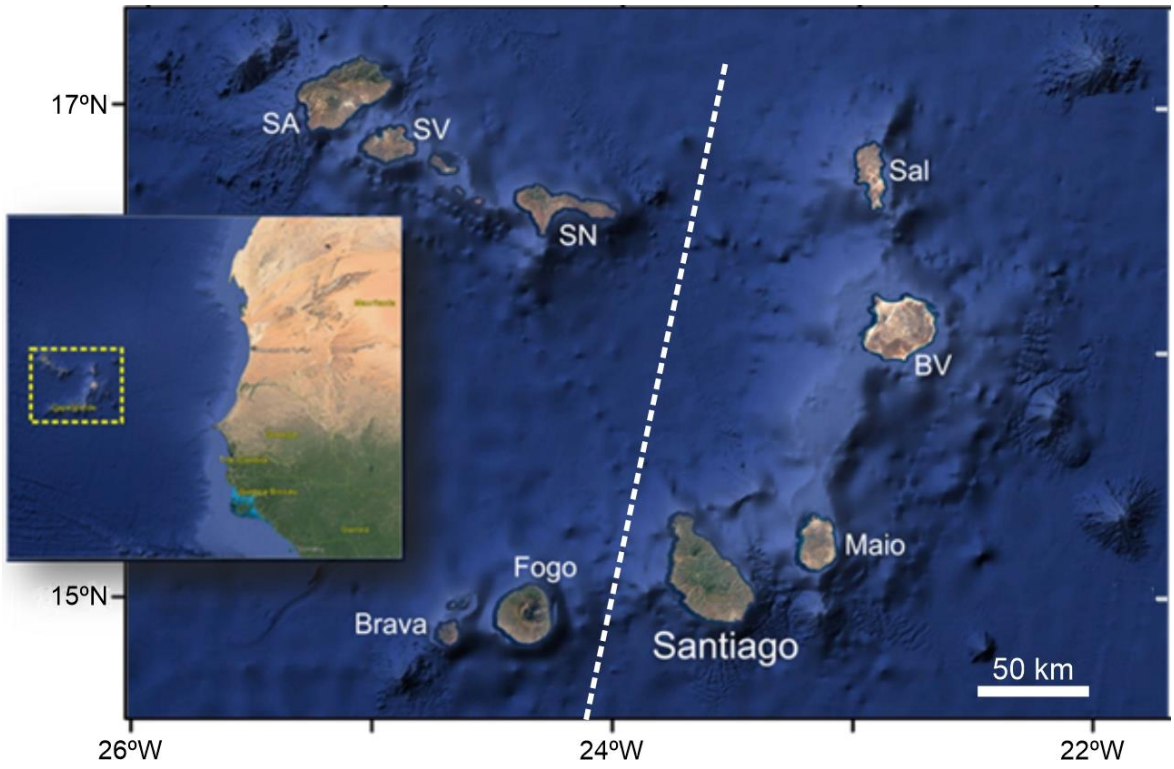

Figure 1. Cape Verde archipelago in the central Atlantic, west of Mauritania and Senegal. The dashed white line marks the location of the MCS Line 3. SA – Santo Antão; SV – São Vicente; SN – São Nicolau; BV – Boavista. Image from Google Earth.

We use Santiago Island in Cape Verde (Fig. 1) as a case study because (1) no flank collapses have yet been recognised there, despite having been recognised in other islands of the archipelago (e.g. Masson et al., 2008), (2) its bean-shape and geological asymmetry hint for an island-scale sector collapse, (3) it comprises a great variety of rock types and deposition environments, and (4) it has superb exposure.

Geological setting

Cape Verde, Madeira, the Canaries and the Azores comprise what is known as

Macaronesia (islands of the blessed or fortunate). The islands in these four archipelagos have undergone large-scale flank collapses: in Madeira (Quartau et al., 2018); in seven islands in the Azores (e.g. Woodhall, 1972; Hildenbrand et al., 2012a, b, 2018, 2024; Costa et al., 2014, 2015; Marques et al., 2018, 2020a, 2021, 2025; Sibrant et al., 2014, 2015a, b, 2016; Weiß et al., 2016); in most of the Canary Islands (Navarro and Coello, 1989; Hurlimann et al., 2000; Urgeles et al., 1998; Carracedo et al., 1999; Krastel et al., 2001; Masson et al., 2002; Mitchell et al., 2002; Hildenbrand et al., 2003; Hunt et al., 2011, 2013; Boulesteix et al., 2012, 2013; Leon et al., 2017) and several Cape Verde islands (e.g. Day et al., 1999; Le Bas et al., 2007; Masson et al., 2008; Marques et al., 2019; Cornu et al., 2021; Samrock et al., 2022). Noticeably, large-scale flank collapses have not been recognised in Santiago Island, Cape Verde, but here we argue that there is good evidence of at least one major sector collapse to the east, and a smaller one to the west. These two old landslides are called sector collapses because they have removed the summit of the volcanic edifice.

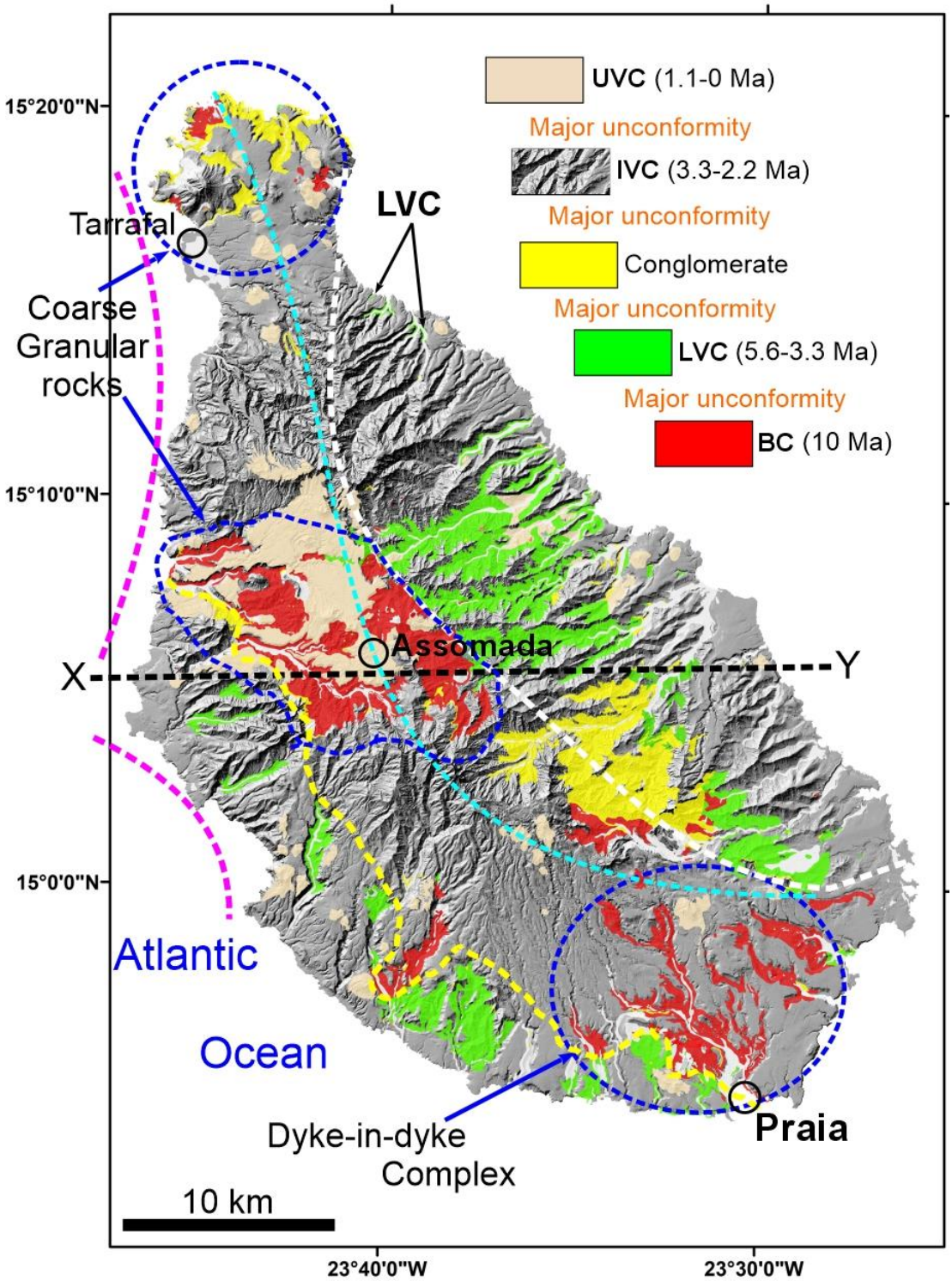

Figure 2. Simplified geological map of Santiago Island overlying the DEM. Dashed blue circles mark the location of the main Basement Complex outcrops and its dominant lithological and

intrusion types: dominant coarse rocks or dominant dyke-in-dyke. The dashed white and yellow lines mark the eastern and western limits of the outcropping Basement Complex (red), respectively, and its unconformable contact with the overlying submarine LVC. The dashed cyan line represents the divide. The dashed magenta lines represent the headwalls of putative large-scale landslides. The X-Y dashed black line marks the location of the geologic profile shown in Fig. 3. BC – Basement Complex; LVC – Lower Volcanic Complex; IVC – Intermediate Volcanic Complex made transparent so that the two more relevant complexes for this work (BC and LVC) stand out; UVC – Upper Volcanic Complex. Geological map simplified and adapted from Serralheiro's (1976) map.

Santiago is the largest of the 10 inhabited islands of Cape Verde (Fig. 1), with the highest altitude reaching 1,394 m at Pico da Antónia. The island is elongated in the NNW-SSE direction and shows rugged topography with large and deep valleys. The volcanic stratigraphy of the island was based on unconformity-bounded stratigraphic units (Serralheiro, 1976) (Fig. 2), but the geological map shows important inconsistencies in terms of volcanic stratigraphy, as already discussed in Holm et al. (2008) and Marques et al. (2020). The volcanic stratigraphy of the island comprises four main volcanic complexes, which were renamed by Marques et al. (2020) to avoid using local names that have no meaning to the common reader.

The volcanic stratigraphy comprises, from bottom to top (Fig. 2):

1. Basement Complex – deeply eroded unit mostly composed of coarse granular rocks (e.g. gabbros and carbonatites) in the centre and northern tip of the island, and a dyke-in-dyke complex in southern Santiago. The Basement Complex represents the deep feeders and magma chambers of an early edifice. Biotite from a foidal gabbro and biotite/phlogopite from carbonatites in the Basement Complex were dated at ca. 10 Ma (Bernard-Griffiths et al., 1975).

2. Lower Volcanic Complex – this unit lies on the Basement Complex through a major unconformity, and is, according to current knowledge, exclusively composed of submarine lavas

111 that outcrop from current sea level to an altitude of ~410 m. According to isotopic ages reported
112 in Holm et al. (2008), Ramalho et al. (2010) and Marques et al. (2020), this thick submarine
113 complex formed between, at least, ca. 5.6 and ca. 3.2 Ma.

114 3. Intermediate Volcanic Complex – this unit overlies the Basement Complex and the Lower
115 Volcanic Complex through major unconformities, in places with an intervening thick
116 conglomerate, and is composed of subaerial flows that pass into submarine flows close to the
117 current coast. This unit was dated in the range 3.3 to 2.2 Ma (Holm et al., 2008; Ramalho et al.,
118 2010).

119 4. Upper Volcanic Complex – similarly to Holm et al. (2008) and Marques et al. (2020), we
120 consider the volcanism younger than 1.1 Ma as one single main volcanic complex. The latter is
121 mostly composed of thick lava flows lying unconformably on all older units through a surface
122 with prominent relief (unconformity). Similarly to the Intermediate Volcanic Complex, subaerial
123 flows pass into submarine flows close to the current coast. The lavas of this complex formed
124 between ca. 1.1 and 0.8 Ma (Holm et al., 2008; Marques et al., 2020). Strombolian cones lie
125 unconformably on all previous units, thus representing the latest episode of volcanism, which is
126 younger than ca. 0.4 Ma.

127 Santiago has experienced significant vertical movements, which are reported in Ramalho
128 et al. (2010) and Marques et al. (2020). The highest altitude where we found submarine lavas of
129 the LVC was ca. 410 m, for which two explanations are possible: the sea level has dropped by
130 that amount since ca. 6 Ma ago, or the island has uplifted by at least 410 m in the same period.
131 The available sea level curves (e.g. Miller et al., 2005) indicate that such large changes have not
132 occurred in the last 10 Ma, therefore, the most likely explanation is island uplift to bring
133 submarine rocks to 410 m altitude. Given that we do not know the depth of lava deposition in the

sea, the 410 m elevation is a minimum.

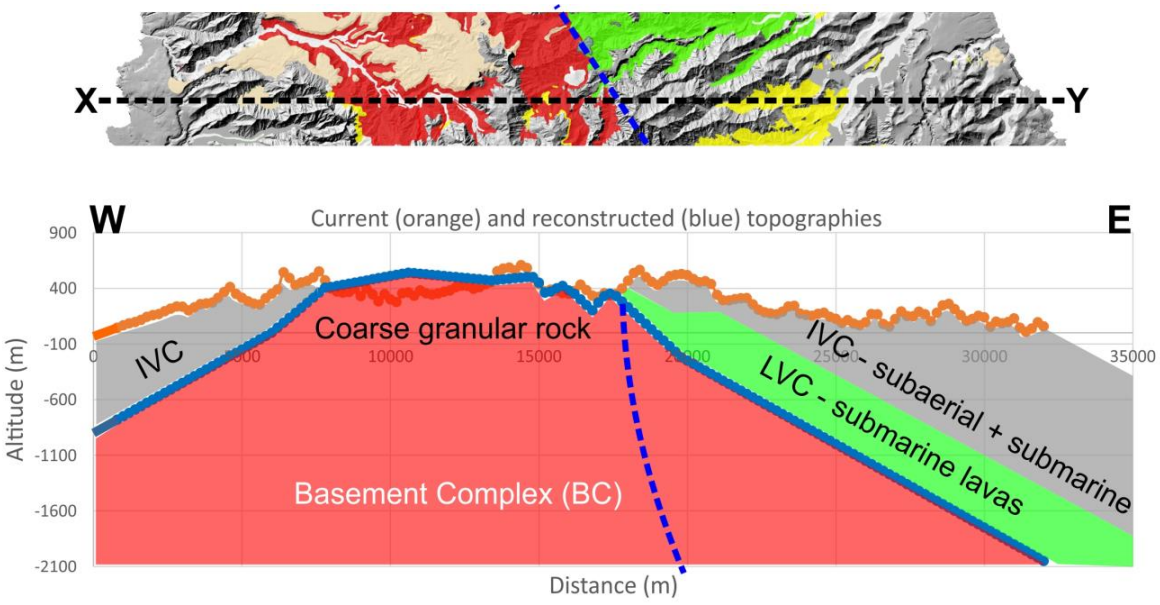

Figure 3. Example of restoration of the BC's topography before the deposition of the submarine complex (> 6 Ma). The profile is also a geological cross-section representative of the structure of the island. Where the BC outcrops, the blue line must be above the orange line; conversely, where the BC is covered by the submarine complex and younger lavas, the blue line must be below the orange line. The slope of the blue line at both E and W ends must be consistent with the current topography and dip at least 8°, as explained in the main text. If the collapse did occur before 6 Ma, then the palaeotopography should be represented by the dashed blue line. The top panel shows a slice of the geological map where the topographic and geological profiles were executed along the dashed X-Y line (see Fig. 2 for location). Note the great difference in thickness of LVC and IVC (Lower and Intermediate Volcanic Complexes, respectively) on opposite flanks of the island. Note that both orange and blue profiles are made up of dots spaced 200 m apart. Vertical exaggeration ≈ 3.7.

Methods

To reconstruct the palaeotopography at the time the submarine complex started covering the Basement Complex, i.e. ca. 6 Ma ago, we used the current DEM and the geological map. Both layers were inserted into QGIS (open-source GIS software) and georeferenced in the same

cartographic reference system, namely WGS_1984_UTM_Zone_27N (EPSG:32627). On the geological map, we plotted a grid of E-W straight lines spaced ca. 1 km apart, which was not always regularly spaced because we wanted to cross as much of the BC as possible. We extracted points every 200 m along the profiles and searched for contacts between the BC and younger volcanic complexes (Fig. 2). To recover the old topography, it was necessary to analyse profile by profile, in detail. To this end, we exported the points of each individual profile, together with their geographical coordinates, lithological class to which they belong and their elevation, to Excel software. The profiles with current topography (orange line in Fig. 3) and outcropping volcanic complexes were recreated on Excel software, where the palaeotopography (blue profile) could be drawn arbitrarily. Therefore, how did we choose the slope angle of the palaeotopography below the volcanic complexes younger than the BC? We had two end-member alternatives: (1) assume that the flank collapse is a fact and, therefore, use a slope angle typical of a normal fault (dashed blue line in Fig. 3), i.e. with a curved shape (listric), where the headwall is steep (>60º) and the slope gradually decreases toward the base. However, this would be a biased solution. (2) To avoid prejudice, we used a very conservative approach, which is to attribute a slope angle to the erosion surface of the buried BC that is similar to the current slope of the submarine island, thus guaranteeing consistency with the geological map (cf. Figs. 3 and 4). Having chosen the conservative and unbiased option, the palaeotopography was built as follows (Figs. 3 and 4): where the BC outcrops, the palaeotopography (blue line) must be above the current topography (orange line); otherwise, the palaeotopography must be below the current topography. Considering that the current slopes of the subaerial and submarine edifice are ca. 3º and 8º on average, respectively, then the recovered slope of the BC should not dip less than 3º and 8º (Fig. 4), otherwise they would be inconsistent with both geology and topography.

Geomorphological analyses on currently active volcanic islands and extra-terrestrial shield volcanoes have shown that subaerial and submarine constructional slopes show a typical angular difference of around 15° (Hildenbrand et al., 2023). On older islands (including Santiago), the former transition from subaerial to submarine (pillow-bearing) lavas carried to the surface by recent uplift consistently shows a similar marked angular difference (Marques et al., 2020a, b). We also note that, at the time of deposition of the submarine complex, the BC was submerged up to the current 410 m altitude, because this is the highest altitude where we currently find submarine lavas (Ramalho et al., 2010; Marques et al., 2020, also for the uplift ages and rates). If the destruction of the BC's edifice was caused by major flank collapse to the east, then the recovered slope should be much steeper than 8º (or even >20° closer to the island), which means that the recovered palaeotopography here presented is very conservative. From the last east and west BC outcropping points, the palaeoslope therefore dips 8º (Fig. 4).

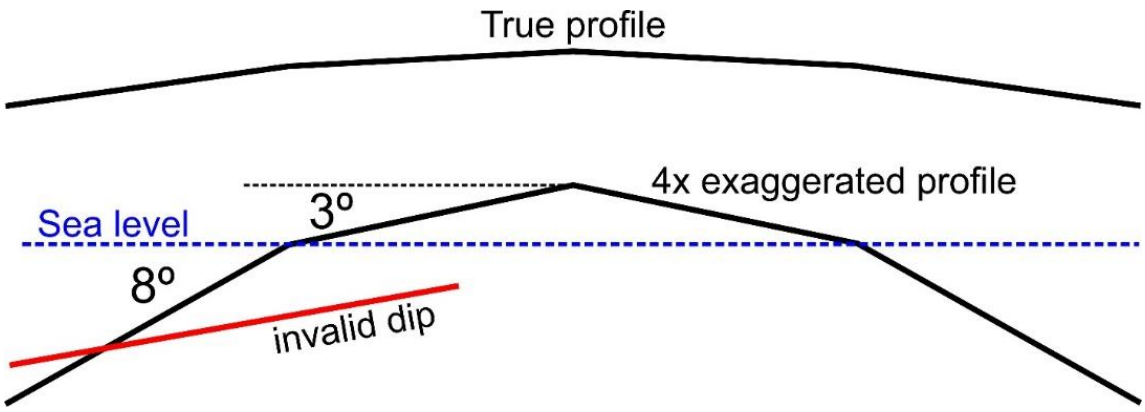

Figure 4. Schematic topographic profiles of Santiago without (top) and with (bottom) vertical exaggeration for easier visualisation of the problem of choosing dip when recovering the palaeotopography. Above sea level, the average slope is ca. 3º, and below sea level is at least 8º. As shown by the red line, the dip cannot be less than 8º, otherwise it crosses the slopes of the volcanic edifice.

The restoration of the old topography was not done automatically; it was done manually, profile by profile, because one must make decisions that the computer is still not able to make by itself without the help of AI, which we do not want to use here. This is particularly true for the BC below the current topography. How steep and how deep is the hidden old topography? These are decisions that we must make on each profile, always taking into consideration the main trends of the neighbouring profiles to avoid undesired artefacts.

Results

Analysis of the geology and palaeotopography

A critical analysis of the geological map of Santiago (Fig. 2) shows important asymmetries: the eastern flank of the island has no outcrops of Basement Complex (BC); if we remove the widespread IVC (as in Fig. 2), Santiago's eastern flank is made up of submarine lavas ca. 5.6-3.3 Ma old that outcrop up to 410 m on this flank; in contrast, on the western flank there are important BC outcrops, and only few LVC submarine lavas that outcrop up to ca. 320 m and are younger (ca. 3.9 Ma) than on the eastern flank; the eastern limit of outcropping BC, i.e. its unconformable contact with the submarine lavas of the LVC (dashed white line in Fig. 2), is markedly concave to the east and stretches almost all of the N-S length of the island. The BC essentially comprises coarse granular rocks and a dyke-in-dyke complex, which means that there has been a large edifice well above the current topography, because the BC is its deep feeding core currently outcropping up to 700 m. The BC at the northern tip of the island comprises essentially granular rocks (mostly gabbro), thus indicating that there has been a main volcanic

centre there too, with important dimensions and summit altitudes well above the current low topography.

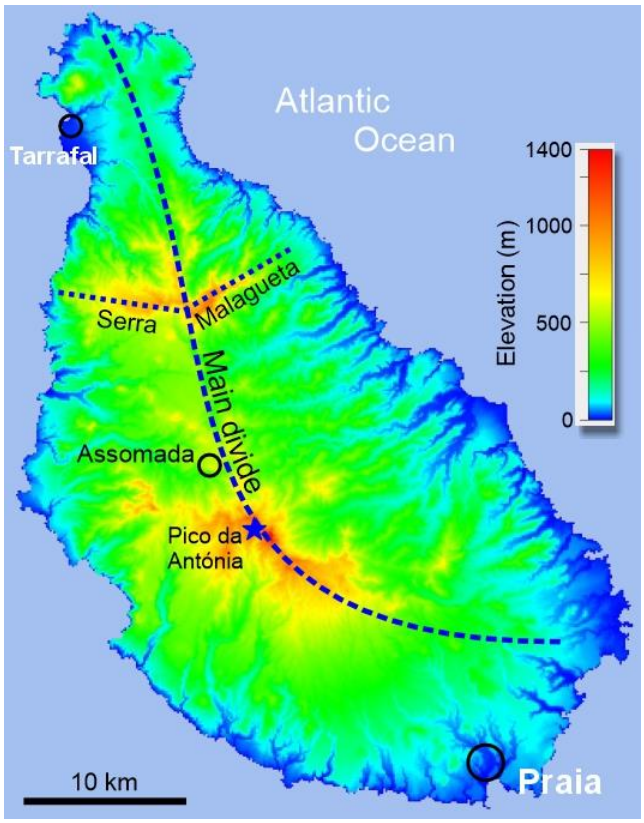

Figure 5. Current Santiago's shaded relief with the dashed blue line marking the main divide of the island. Pico da Antónia (1392 m altitude) and Serra da Malagueta (1064 m) are the main topographic reliefs. Note that, even today and despite deposition of all volcanic complexes above the Basement Complex, the main divide is still conspicuously concave to the east, thus indicating deposition of lavas < 6 Ma old on an island-scale unconformity concave to the east, which has not been fully filled by the younger volcanism. The dotted blue line represents a secondary divide.

The current DEM shows two main topographic reliefs, Pico da Antónia (1392 m) and Serra da Malagueta (1064 m), and a main divide running approximately NNW-SSE, with inflexion to the east in the south (Fig. 5). Analysis of the current DEM shows major

asymmetries: (1) the island is bean-shaped, with the western coast markedly convex to the west; (2) despite the deposition of all volcanic complexes above the BC (ca. 6 Ma of lava flow pilling), the main divide is still conspicuously concave to the east; (3) Serra da Malagueta separates a southern large bean-shaped island from a northern much smaller and circular part of the island, the Tarrafal region (Fig. 5), both connected by a neck made by embayments (seemingly more pronounced to the east because Tarrafal sits on a very young lava delta). All these asymmetries in geology and topography hint at an island-scale collapse to the east and smaller, though still large, flank collapses to the west (magenta lines in Fig. 2).

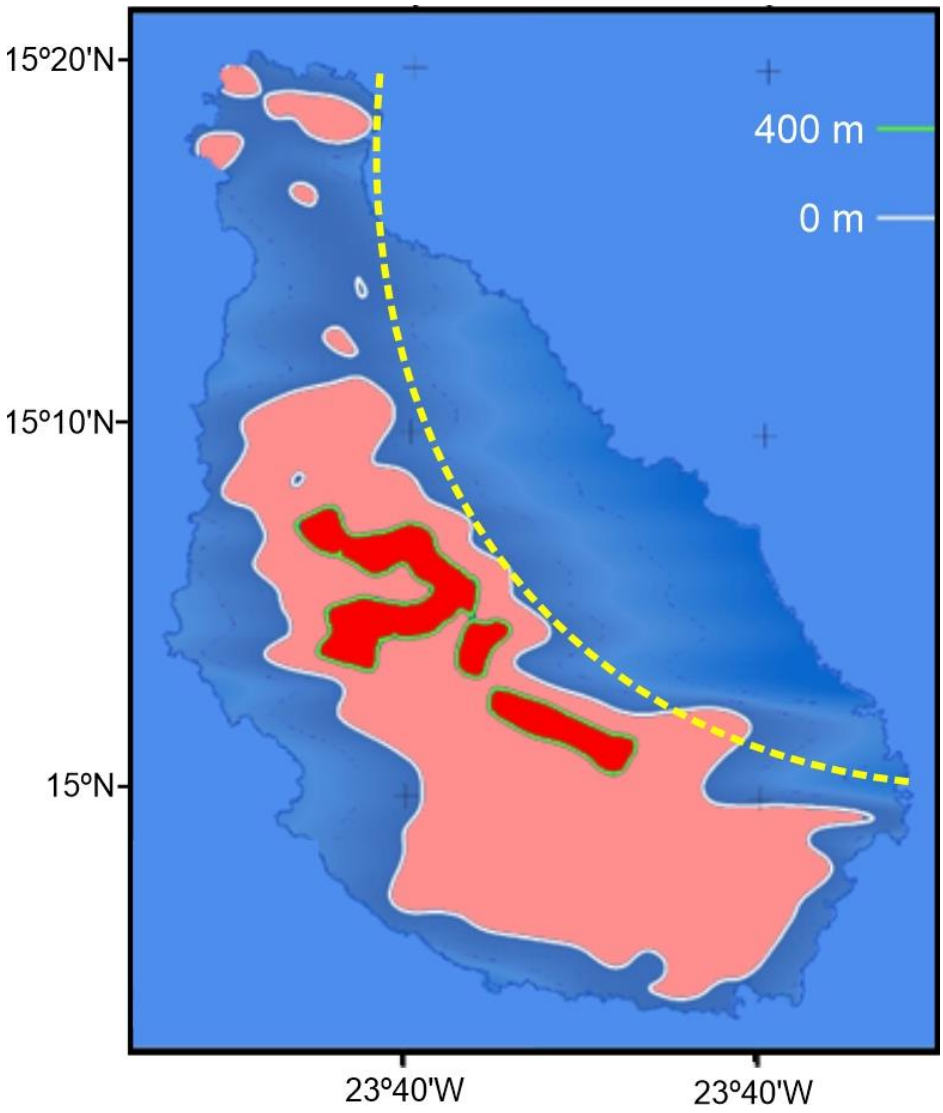

Figure 6. Basement Complex palaeotopography pasted on the current shaded relief. The Basement Complex palaeotopography is shown down to current sea level (light red areas delimited by white line), and above 400 m altitude (red areas delimited by green line) to show the palaeoisland when the submarine lavas of the Lower Volcanic Complex were deposited. Santiago Island would have looked like the red areas 6 Ma ago, and would look currently like the light red area if no younger volcanics had deposited on top of the Basement Complex. The dashed yellow line follows the unconformable contact between BC and LVC, thus representing the headwall of the inferred collapse.

Location and size of shield volcanoes on an early island

Following the reconstruction process, we built a DEM of the palaeotopography by importing the points of each profile into QGIS again, but now with their new simulated elevation values. These elevations were then interpolated between neighbouring profiles, using a minimum curvature spline, and producing a DEM with 50x50 m pixel size. The final result is shown in Figs. 6 and 7 for the current (0 m) and ca. 6 Ma old (ca. 400 m) sea levels.

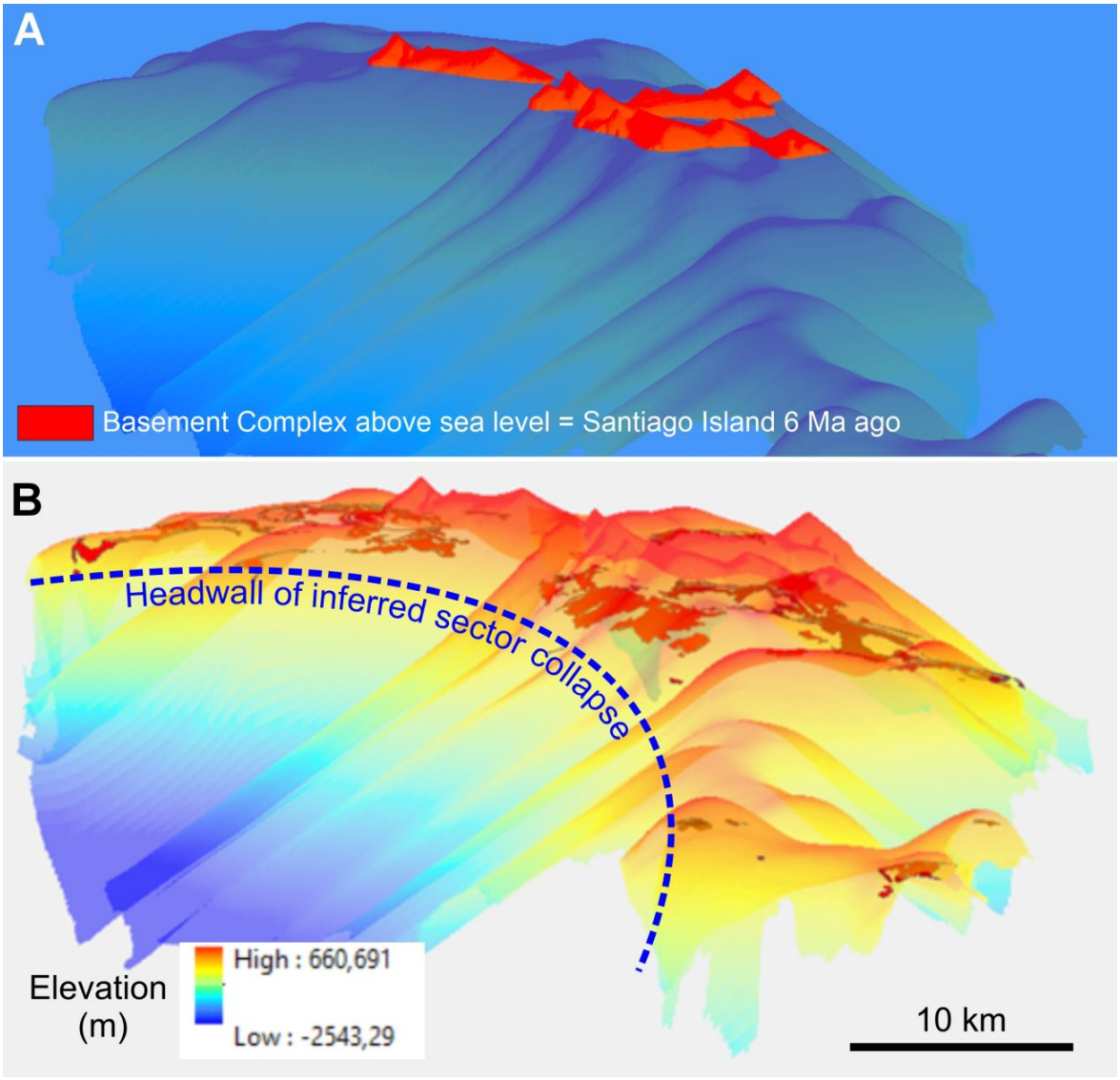

Figure 7. 3-D shaded relief of the recovered Basement Complex palaeotopography viewed from the north. The red areas in A correspond to the Basement Complex above 400 m altitude, i.e.

Santiago Island at ca. 6 Ma, when the submarine lavas (Lower Volcanic Complex) were being deposited unconformably on the Basement Complex. The red areas in B correspond to the currently outcropping Basement Complex. The dashed blue line marks the headwall of the inferred sector collapse that occurred before 6 Ma. Even using a very conservative palaeoslope, the morphology of eastern Santiago is conspicuously concave to the east at the scale of the entire island. Vertical exaggeration = 2x.

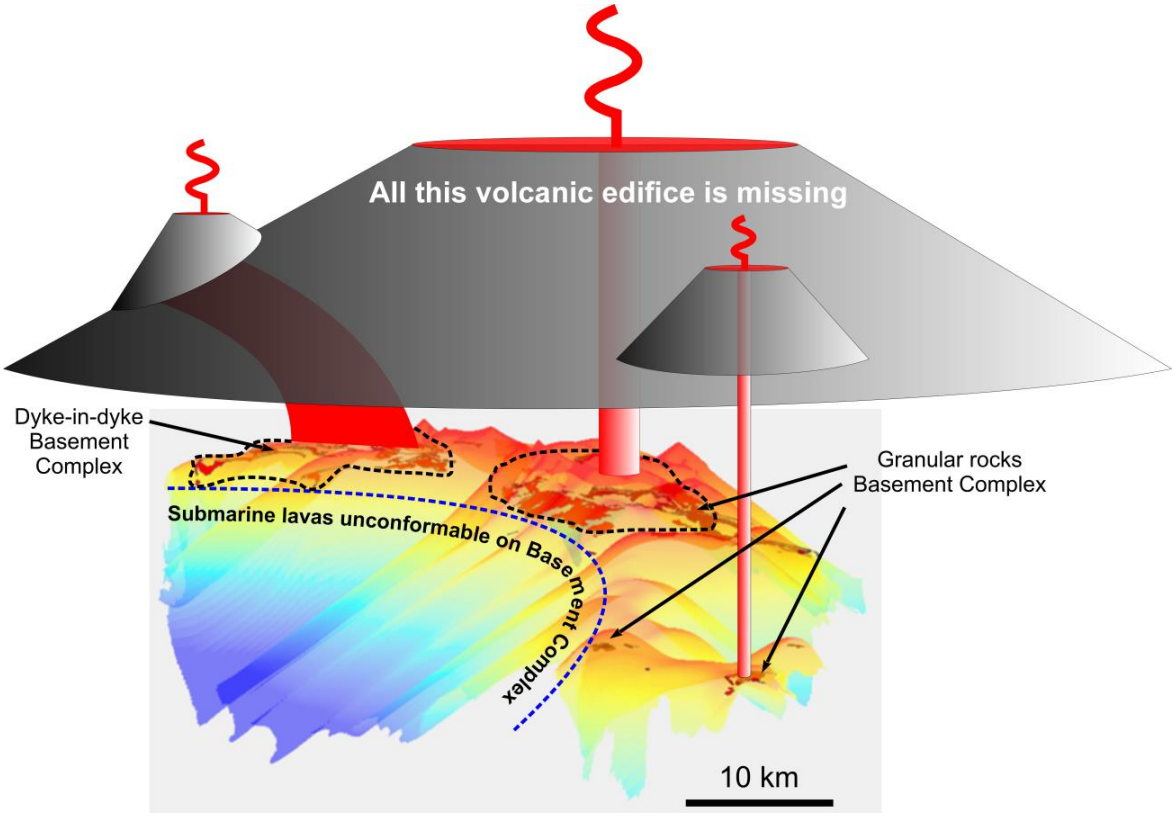

Figure 8. 3-D shaded relief of the recovered palaeotopography down to -2,500 m depth. View from the NE. The island-scale eastward concave shape of the topography before the deposition of the submarine complex is conspicuous and calls for an explanation. Note that the Basement Complex comprises the substratum where the old topography was carved, and, from the deep-seated nature of its rocks, we can infer that at least one volcanic edifice peaking well above the current topography must have existed before destruction.

Supported by the reconstruction shown in Fig. 7B, together with the geological data, we could draw the likely volcanic morphology represented in Fig. 8.

Volume of missing rocks

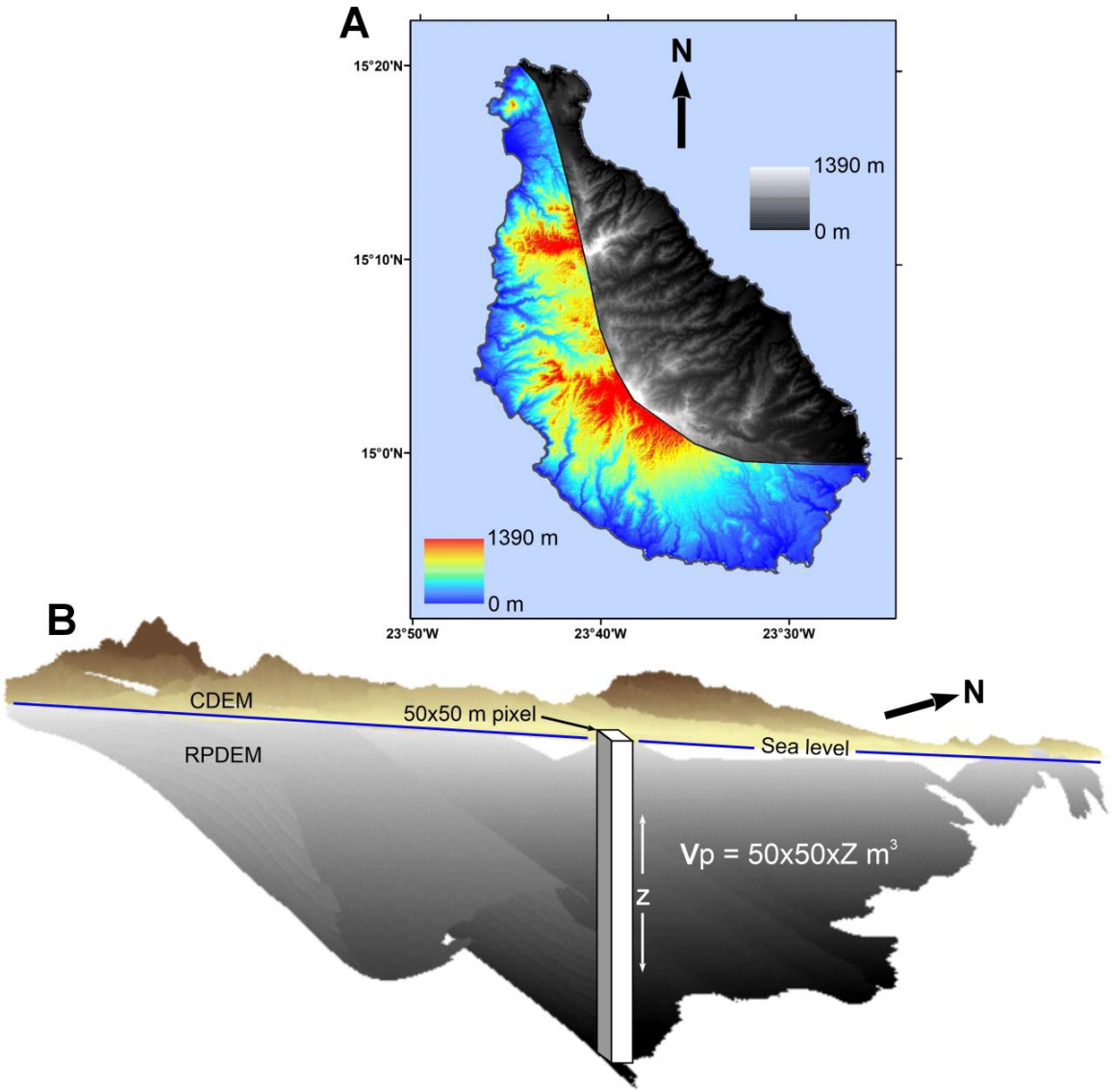

Figure 9. Sketch to illustrate how we estimated the volume of rock missing between the basement and the current topography, which is only a small fraction of what is actually missing, considering the removed edifice on and offshore (cf. Fig. 8). A – current DEM where the grayscale area corresponds to the inferred collapsed sector, which is used in B to show how we estimated the minimum volume of missing rock. B – sketch to illustrate how we estimated the minimum volume of rock removed by the sector collapse. We find the difference in altitude (Z) between the current DEM (CDEM) and the restored palaeotopography DEM (RPDEM), and multiply by the area of each 50x 50 m pixel (pixel volume = Vp = 50x50xZ m^3). The total volume

285 *is the sum of all individual pixel volumes.*

286

287 Thanks to the method developed here, we can estimate the minimum onshore volume of
288 rock involved in the sector collapse. The methodology we followed is illustrated in Fig. 9. We
289 start by finding the difference in altitude (Z) between the current DEM and the restored
290 palaeotopography DEM, and multiply Z by the area of each 50x50 m pixel: pixel volume = Vp =
291 50x50xZ m^3). Finally, the total volume is calculated by summing up all individual pixel
292 volumes. The estimated volume is ca. 370 km^3, which is a minimum because the estimated
293 volume lies between the current topography and the reconstructed palaeotopography before 6
294 Ma, and within the current island (i.e. onshore). Ideally, the volume should encompass the
295 missing summit and subaerial and submarine flanks of the pre-6 Ma volcano, which was much
296 larger in height and, likely, radius than the current topography (cf. Fig. 8), but whose original
297 shape we do not know.

298

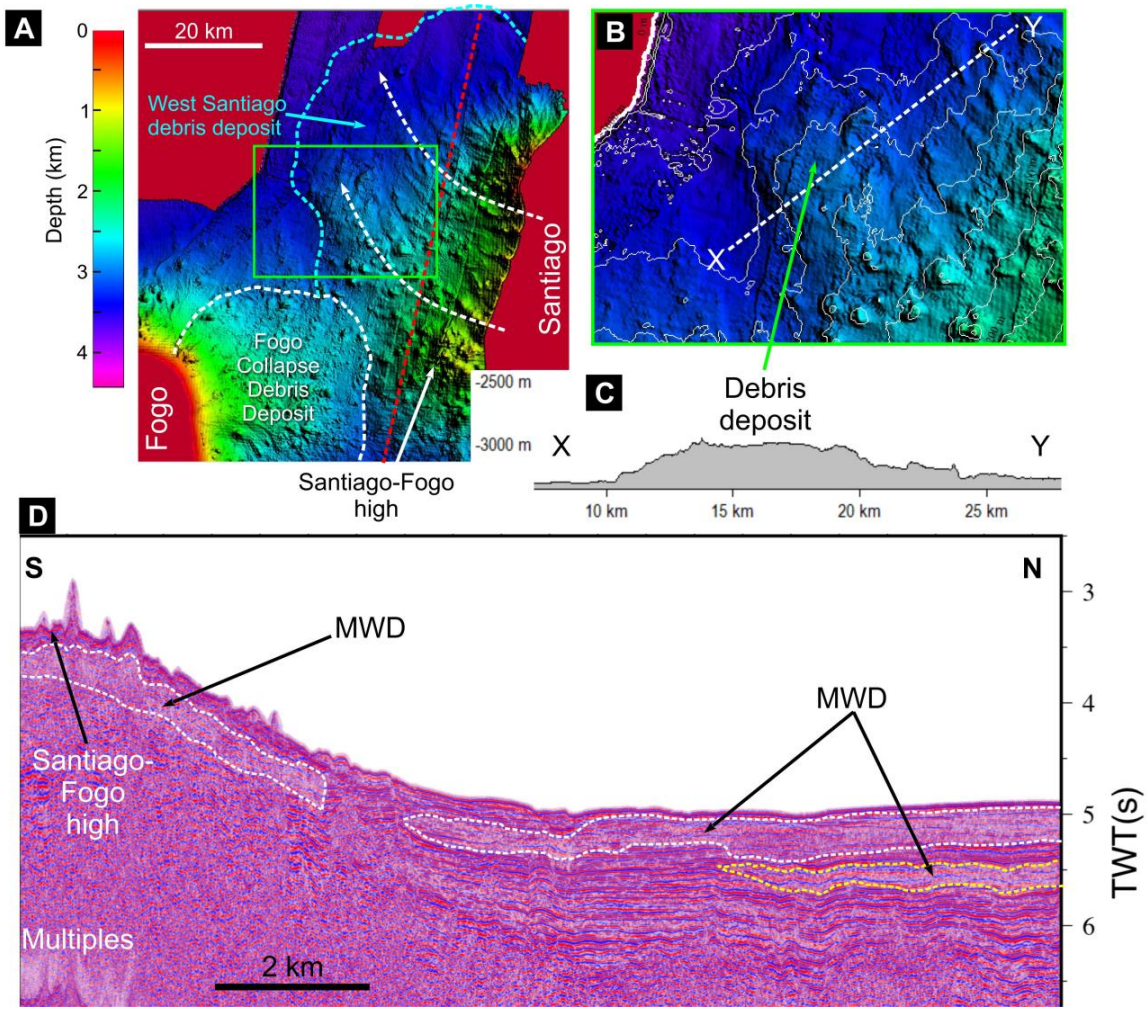

Figure 10. Bathymetric and seismic images used in this work. A – shaded relief of the bathymetry with delimitation of the interpreted mass wasting deposits (MWD) west of Santiago. B – zoom of the green rectangle in A to show the km-scale tongue convex to the NW, which we identify as a typical landslide feature. C – topographic profile of the tongue identified in B, to show the thick interpreted debris deposit resulting from a slide down the western slope of Santiago toward the NW.

Marine geophysics

Despite eastern Santiago being the focus of the present study, we use data from the west as analogue of the inferred collapse in the east because it is a good example of landsliding

310 associated with debris deposits and conspicuous half-moon scars on western Santiago (Fig. 2),
311 which help to support our inference of sector collapse on eastern Santiago in the absence of
312 seismic data here. Here, we use data from the Southampton Oceanography Centre, provided by
313 the British Oceanographic Data Centre. Data were collected during RRS Charles Darwin Cruise
314 CD168 between 02 and 16 February 2005. We could only have access to multichannel seismic
315 data west of Santiago because, apparently, there are no data in the east. .

316 The bathymetry between Santiago and Fogo islands (Fig. 10A) shows the debris deposit
317 identified by Masson et al. (2008) and related to the east Fogo collapse. Interpretations of the
318 bathymetry (Fig. 10A to C) and multichannel seismic Line 3 (Fig. 10D) indicate the existence of
319 mass wasting deposits (MWD in Fig. 10D) west of Santiago. The interpretation of MWDs in the
320 seismic line is mostly based on the seismic transparency of some layers, their shapes and the
321 erosive character of their bases. The interpretation of MWDs from the bathymetry west of
322 Santiago is based on the shape (westward concave embayments) of the island above sea level (cf.
323 magenta dashed lines in Fig. 2), the chaotic character of reflector bodies on the seismic line, and
324 the well-preserved km-scale tongue well visible on the bulging bathymetry, both in plan and
325 cross-section views (Fig. 10B and C, respectively). The bulge in the bathymetric contours on the
326 western submarine slope of Santiago (in contrast to the shape of the island above sea level)
327 suggests an area of landslide debris deposits, which are smoother (younger sediment cover) than
328 the Fogo debris deposit and are dissected by canyons, thus suggesting a relatively older feature.

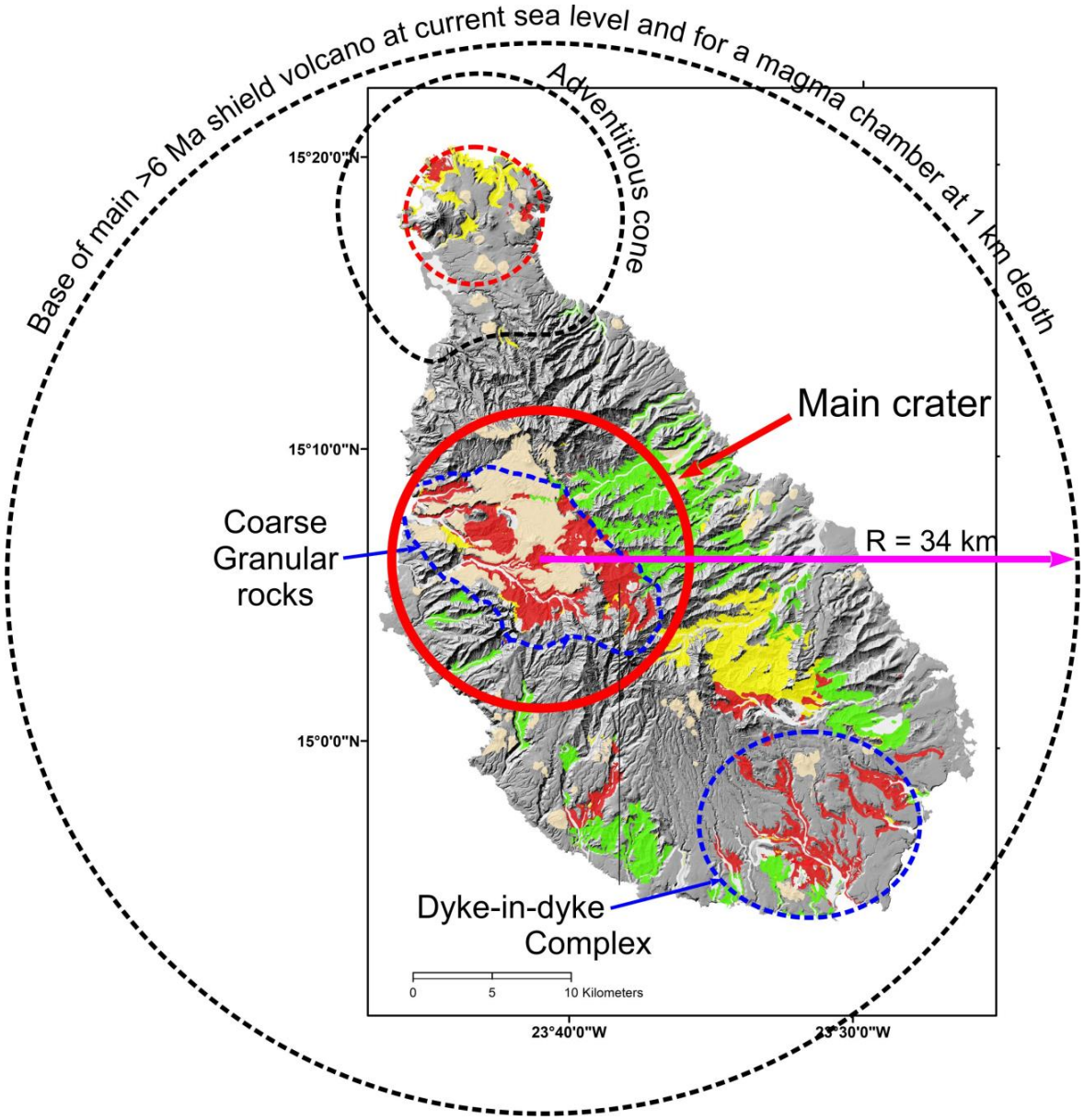

329

330 *Figure 11. Sketch drawing on the simplified geological map to show how we constrained the*
331 *maximum size of the shield volcano older than 6 Ma. Note that the dyke-in-dyke complex must lie*
332 *inside the circle representing the volcano, and that the granular rocks representing the volcano*
333 *core should lie below the main crater. Simple trigonometry shows that, for a radius of 34 km, the*
334 *height of the destroyed volcano should be ca. 1800 m, and the depth of the top of the granular*
335 *rocks ca. 1000 m.*

336

Discussion and conclusions

General implications

Santiago's volcanic stratigraphy and rock distribution show good evidence for the existence of an early island composed of two volcanic cones centered where the coarse granular rocks currently outcrop (assuming that they represent feeder magma chambers)(Fig. 8): a main subaerial shield volcano and two smaller cones at the southernmost and northernmost regions of the island. If the core of the old central volcano currently peaks at ca. 700 m altitude, then the old volcano must have peaked at a much higher altitude, depending on the depth at which the granular rocks formed. The depth of magma chambers is not consensual, but Santiago could be an interesting case study in this respect. Assuming that the optimal depth of subvolcanic magma chamber growth is around 6 km (Huber et al., 2019), then we can try to calculate how much of the early island might be missing. However, this number is unrealistic, because if we add 6 km to 4 km of edifice below sea level and to the 300 m peak altitude of the Basement Complex above the submarine complex (total 10.3 km), then Santiago would have been as tall as the largest mountain on Earth, which is the Big Island in Hawaii. On the other hand, if we assume that the missing volcano was subaerial, with a typical 3º flank slope of a basaltic shield volcano, and the main crater vertically above the granular rocks, then its height is constrained by the radius of its base. In Santiago the radius is constrained by the position of the dyke-in-dyke complex (Fig. 11), which must lie inside the shield. Simple trigonometry (tan3º = altitude/34 km radius at current sea level) yields ca. 1800 m volcano height, which means that the topmost granular rocks below the main crater crystallised at ca. 1100 m depth (1800 m – 700 m of the current maximum altitude of the BC). Note that we have drawn the base of the sub-aerial edifice relatively close to the dyke-in-dyke complex (cf. Fig. 11),

360 therefore, the estimates above are conservative. However, the base of the hypothetical edifice is
361 too far from the current island shoreline everywhere except in the south, which means that
362 something is not right in the reasoning used. At least four explanations are likely: (1) we did not
363 take into account that the island has been uplifted by at least 400 m, which would make the radius
364 at the current sea level significantly smaller (radius = altitude/tan3º = (1800 – 400) /tan3º ~ 27
365 km); (2) we used a slope of 3º, but it could be more, so making the basal radius much smaller, even
366 without taking into account island uplift (radius = altitude/tan5º = 1800/tan5º = 21 km radius at
367 current sea level), which would put the dyke-in-dyke complex out of the edifice; (3) the
368 outcropping granular rocks in the middle of the island, which we assumed to represent a magma
369 chamber vertically below the main crater, might be significantly deviated from the vertical of the
370 main crater, thus guaranteeing that the dyke-in-dyke complex sits within the older edifice despite
371 having a smaller radius; and (4) the former main island was not a single large shield with a unique
372 magma chamber; instead, it could have been a linear volcanic ridge comprising coalescent
373 volcanic edifices, similarly to what has been found in the Azores (e.g., Hildenbrand et al., 2008;
374 2014; Sibrant et al., 2015b; Marques et al., 2021, 2025).

375 The sedimentation rate in the region of the Cape Verde islands can be estimated from
376 data in Ali et al. (2003; mainly their Figs. 2 and 7). It is in the order of 0.015-0.019 mm/a (ca. 2
377 to 2.5 km/130 Ma, the age of the oceanic crust below Santiago), which is in the same order of
378 magnitude as the sedimentation rate found in the Azores (ca. 0.023 mm/a), although with more
379 volcanic input here (cf. Beier et al., 2022; Marques et al., 2025). This means that a mass-wasting
380 deposit 6 to 8 Ma old would be covered by ca. 100 m of sediment. This is consistent with the thin
381 veneer of sediment covering the mass-wasting deposit inferred in the seismic line (Fig. 10D).
382 The position of the inferred mass-wasting deposit is also consistent with the position of the large-

scale embayments observed in western Santiago (magenta lines in Fig. 2).

Causes for the missing rocks

Whatever the exact size and position of the older volcano, one thing is clear: a very large volume of rock is missing, which begs for an explanation. We are aware of the main processes that can remove rock from an oceanic island, but these are typically slow and produce a growing marine shelf around the island. However, the expected wide shelf does not exist around Santiago, nor have we found evidence that it has existed in the past. Santa Maria Island in the Azores is a good example of the expected cumulative effects of meteoric and marine erosion, and large-scale edifice removal by sector collapses (Sibrant et al., 2015a; Marques et al., 2020a, 2025). In Santa Maria, volcanism has been extinct since 2.8 Ma, but the island has survived well from meteoric and marine erosions. This means that this kind of rock removal is not enough to justify the rapid disappearance of a large part of a massive volcano, to the point of exposing its roots (magma chamber) as in Santiago. A large number of coalescing small collapses, which is the same as saying normal coastal retreat by marine erosion, would hardly (if ever) produce the island-scale eastward concave shape of Santiago, and even less be able to remove the full edifice above the granular rocks that represent the core (magmatic chamber) of the older volcanic edifice.

Morphological, current and past (>6 Ma), and geological evidence all point to the existence of an island-scale eastward-directed sector collapse. It is very clear from the geological map (Fig. 2) and geological profile (Fig. 3) that the distribution and thickness of the volcanic complexes over the Basement Complex are markedly asymmetric between eastern and western Santiago. If the eastern BC's slope is actually a collapse scar (dashed blue line in Fig. 3), then its

405 dip is much steeper, and the asymmetry becomes even greater.

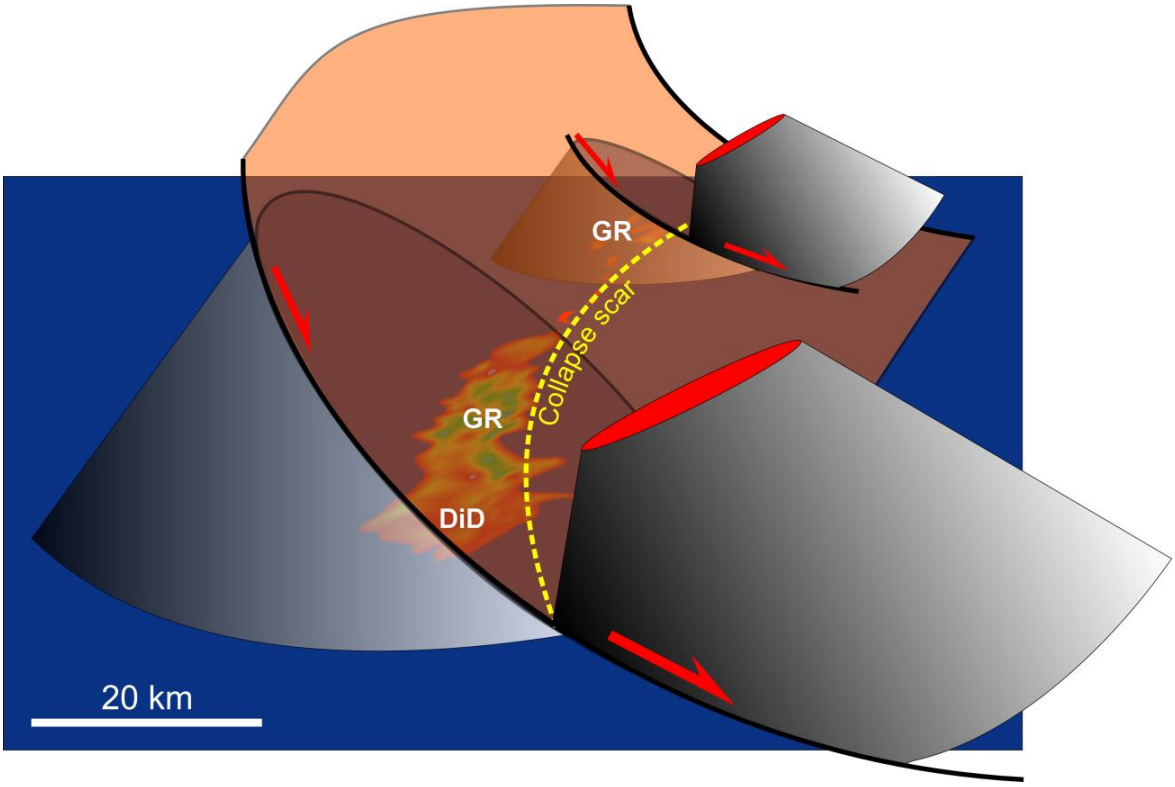

406

407 *Figure 12. Sketch drawing over recovered palaeotopography in the background to illustrate the*
408 *inferred eastward flank collapse that affected the two volcanoes comprising the Basement*
409 *Complex before the start of deposition of the submarine complex ca. 6 Ma ago. The collapse*
410 *involved the summit and one flank, therefore, we call it a sector collapse.*

411

412 *Model of the sector collapse (Fig. 12)*

413 The inferred island-scale sector collapse can be envisaged as represented in Fig. 12. The
414 island older than 6 Ma was much larger than the present-day island (cf. Fig. 11), became
415 gravitationally unstable, and collapsed. The basal fault cut deep into the core of the volcanic
416 edifice, i.e. through the magma chambers represented by the granular rocks, which means that a
417 large volume of rock was removed (summit and whole eastern flank).

Regarding the collapse speed (catastrophic = fast vs. slump = slow), we note that Santiago's edifice lies very close to Maio's edifice, whose granular rocks have ages similar to Santiago's (Samrock et al., 2022). Given the position of Santiago relative to the nearby Maio Island (cf. Fig. 1), which could work as a buttress in the east, we conclude that the debris generated by the inferred eastward collapse might have been diverted to the northeast. Interestingly, Samrock et al. (2022) recognised a tsunami deposit between 6.7 and 8.7 Ma on the neighbouring Maio Island, which faces eastern Santiago, with an age fitting the age of the sector collapse we have now recognised in Santiago, i.e. between 6 and 10 Ma. Therefore, we conclude that it was fast enough to produce the tsunami deposit identified by Samrock et al. (2022) on Maio Island.

Putting together (1) the island scale erosion to show the deep feeders currently at the surface and up to 700 m asl, (2) the eastward concave shape of the unconformable contact between the BC (>10 Ma) and the LVC (<6 Ma), (3) the current shape of the divide (mostly concave to the east), and (4) the mass wasting deposits in the west inferred from both the bathymetry and the seismic data (indirect evidence), it seems to us enough to be a good hint on the kind of erosion that massively destroyed the original edifice (Fig. 12). Having ruled out possible explanations such as meteoric and marine erosions, we conclude for a sector collapse as the only plausible explanation

Santiago's case and the methodology used here for the restoration of a palaeotopography could be used as examples for the study of many islands worldwide where granular rocks are currently at the surface, and sometimes at significant altitude.

Acknowledgements

We thank the Southampton Oceanography Centre and the British Oceanographic Data Centre for providing the bathymetric and seismic data used in this work. C.M. Catita's contribution was funded by the Portuguese Foundation for Science and Technology, FCT, I.P./MCTES through national funds (PIDDAC): UID/50019/2025 and LA/P/0068/2020 https://doi.org/10.54499/LA/P/0068/2020).

References

Ali, M.Y., Watts, A.B., Hill, I., 2003. A seismic reflection profile study of lithospheric flexure in the vicinity of the Cape Verde Islands. J. Geophys. Res. 108, 2239.

Beier, C. et al., 2022. The submarine Azores Plateau: evidence for a waning mantle plume? Marine Geology 451, 106858.

Bernard-Griffiths, J., Cantagrel, J.M., Alves, C., Mendes, F., Serralheiro, A., Macedo, J., 1975. Geochronologie: Données radiometriques potassium/argon sur quelques formations magmatiques des îlles de l'archipel du Cap Vert. Comptes Rendus des Seances de l'Académie des Sciences, D280, 2429–2432.

Boulesteix, T., Hildenbrand, A., Gillot, P.Y., Soler, V., 2012. Eruptive response of oceanic islands to giant landslides: New insights from the geomorphologic evolution of the Teide–Pico Viejo volcanic complex (Tenerife, Canary). Geomorphology 138, 61-73.

Boulesteix, T., Hildenbrand, A., Soler, V., Quidelleur, X., Gillot, P. Y., 2013. Coeval giant landslides in the Canary Islands: Implications for global, regional and local triggers of giant flank collapses on oceanic volcanoes. Journal of Volcanology and Geothermal Research 257,

462 90-98.

463 Carracedo, J.C., Day, S.J., Guillou, H., Torrado, F.J.P., 1999. Giant Quaternary landslides in the
464 evolution of La Palma and El Hierro, Canary Islands. J. Volcanol. Geotherm. Res. 94, 169-
465 190.

466 Cornu, MN., Paris, R., Doucelance, R. *et al.*, 2021. Exploring the links between volcano flank
467 collapse and the magmatic evolution of an ocean island volcano: Fogo, Cape Verde. Sci
468 Rep 11, 17478.

469 Costa, A. C. G., Hildenbrand, A., Marques, F. O., Sibrant, A. L. R., Santos de Campos, A., 2015.
470 Catastrophic flank collapses and slumping in Pico Island during the last 130 kyr (Pico-Faial
471 ridge, Azores Triple Junction). Journal of Volcanology and Geothermal Research 302, 33-46.

472 Costa, A.C.G., Marques, F.O., Hildenbrand, A., Sibrant, A.L.R., Catita, C.M.S., 2014. Large-
473 scale catastrophic flank collapses in a steep volcanic ridge: The Pico-Faial Ridge, Azores
474 Triple Junction. Journal of Volcanology and Geothermal Research 272, 111-125.

475 Day, S., Heleno da Silva, S.I.N., Fonseca, J.F.B.D., 1999. A past giant lateral collapse and
476 present day flank instability of Fogo, Cape Verde Islands. J. Volcanol. Geotherm. Res. 94,
477 191-218.

478 Hildenbrand, A., Madureira, P., Marques, F.O., Cruz, I., Henry, B., Silva, P., 2008. Multi-stage
479 evolution of a sub-aerial volcanic ridge over the last 1.3 Myr: S. Jorge Island, Azores Triple
480 Junction. Earth and Planetary Science Letters 273, 289-298.

481 Hildenbrand A., Weis D., Madureira P., Marques F.O., 2014. Recent plate re-organization at the
482 Azores Triple Junction: evidence from combined geochemical and geochronological data on
483 Faial, S. Jorge and Terceira volcanic islands. Lithos 210-211, 27-39.

Hildenbrand, A., Marques, F.O., Catalão, J., 2018. Large-scale mass wasting on small volcanic islands revealed by the study of Flores Island (Azores). Scientific Reports 8, 13898.

Hildenbrand, A., Marques, F.O., Catalão, J., Catita, C.M.S., Costa, A.C.G., 2012a. Large-scale active slump of the SE flank of Pico Island (Azores). Geology 40, 939-942.

Hildenbrand, A., Marques, F.O., Pereira, A. et al., 2024. Precise dating of large flank collapses by single-grain $^{40}Ar/^{39}Ar$ on pyroclastic deposits from the example of Flores Island (Azores). Sci Rep 14, 11905.

Hildenbrand, A. et al., 2012b. Reconstructing the architectural evolution of volcanic islands from combined K/Ar, morphologic, tectonic, and magnetic data: the Faial Island example (Azores). Journal of Volcanology and Geothermal Research 241-242, 39–48.

Hildenbrand, A., Zeyen, H., Schmidt, F., Bouley, S., Costard, F., Gillot, P.Y., Marques, F.O., Quidelleur, X., 2023. A giant volcanic island in an early Martian Ocean? Earth and Planetary Science Letters. 619, 118302.

Holcomb, R.T., Searle, R.C., 1991. Large landslides from oceanic volcanoes. Mar. Geotech. 10, 19-32.

Holm, P. M., Grandvuinet, T., Friis, J., Wilson, J. R., Barker, A. K., Plesner, S., 2008. An $^{40}Ar/^{39}Ar$ study of the Cape Verde hot spot: Temporal evolution in a semistationary plate environment. Journal of Geophysical Research, 113, B08201.

Huber, C., Townsend, M., Degruyter, W., Bachmann, O., 2019. Optimal depth of subvolcanic magma chamber growth controlled by volatiles and crust rheology. Nature Geoscience 12, 762-768.

Hunt, J.E., Wynn, R.B., Masson, D.G., Talling, P.J., Teagle, D.A.H., 2011. Sedimentological and

506 geochemical evidence for multistage failure of volcanic island landslides: A case study from
507 Icod landslide on north Tenerife, Canary Islands. Geochem. Geophys. Geosyst. 12, Q12007.

508 Hunt, J.E., Wynn, R.B., Talling, P.J., Masson, D.G., 2013. Multistage collapse of eight western
509 Canary Island landslides in the last 1.5 Ma: Sedimentological and geochemical evidence from
510 subunits in submarine flow deposits. Geochem. Geophys. Geosyst. 14, 2159-2181.

511 Krastel, S., Schmincke, H.U., Jacobs, C.L., Rihm, R., Le Bas, T.P., Alibes, B., 2001. Submarine
512 landslides around the Canary Islands. Journal of Geophysical Research 106, 3977-3997.

513 Le Bas, T.P., Masson, D.G., Holtom, R.T., Grevemeyer, I., 2007. Slope failures of the flanks of
514 the southern Cape Verde Islands. In Submarine Mass Movements and Their Consequences,
515 Advances in Natural and Technological Hazards Research, V. Lykousis, D. Sakellariou, J.
516 Locat, Eds. (Springer, Dordrecht, Netherlands), vol. 27, pp. 337-345.

517 León, R., Somoza, L., Urgeles, R., Medialdea, T., Ferrer, M., Biain, A., García-Crespo, J.,
518 Mediato, J.F., Galindo, I., Yepes, J., González, F.J., Gimenez-Moreno, J., 2017. Multi-event
519 oceanic island landslides: New onshore-offshore insights from El Hierro Island, Canary
520 Archipelago. Mar. Geol. 393, 156-175.

521 Maccaferri, F., Richter, N., Walter, T.R., 2017. The effect of giant lateral collapses on magma
522 pathways and the location of volcanism. Nat Commun 8, 1097.

523 Manconi, A., Longpré, M.A., Walter, T.R., Troll, V.R., Hansteen, T.H., 2009. The effects of
524 flank collapses on volcano plumbing systems. Geology 37, 1099-1102.

525 Marques, F.O., Catalão, J., Hübscher, C., Costa, A.C.G., Hildenbrand, A., Zeyen, H., Nomikou,
526 P., Lebas, E., Zanon, V., 2021. The shaping of a volcanic ridge in a tectonically active setting:
527 The Pico-Faial Ridge in the Azores Triple Junction. Geomorphology 378, 107612.

528 Marques, F.O., Hildenbrand, A., Costa, A.C.G., Sibrant, A.L.R., 2020a. The evolution of Santa
529 Maria Island in the context of the Azores Triple Junction. Bulletin of Volcanology 82, 39.

530 Marques, F. O., Hildenbrand, A., Hübscher, C., 2018. Evolution of a volcanic island on the
531 shoulder of an oceanic rift and geodynamic implications: S. Jorge Island on the Terceira Rift,
532 Azores Triple Junction. Tectonophysics 738, 41-50.

533 Marques, F.O., Hildenbrand, A., Victória, S.S., Cunha, C., Dias, P., 2019. Caldera or flank
534 collapse in the Fogo volcano? What age? Consequences for risk assessment in volcanic
535 islands. Journal of Volcanology and Geothermal Research 388, 106686.

536 Marques, F.O., Hildenbrand, A., Zeyen, H., Cunha, C., Victória, S.S., 2020b. The complex
537 vertical motion of intraplate oceanic islands assessed in Santiago Island, Cape Verde.
538 Geochemistry, Geophysics, Geosystems 21, e2019GC008754.

539 Marques, F.O., Ribeiro, L.P., Hübscher, C., Costa, A.C.G., Hildenbrand, A., 2025. How and why
540 small volcanic ocean islands collapse and move vertically up and down. Nature Scientific
541 Reports 15, 3835.

542 Masson, D.G., Le Bas, T.P., Grevemeyer, I., Weinrebe, W., 2008. Flank collapse and large-scale
543 landsliding in the Cape Verde Islands, off West Africa. Geochem. Geophys. Geosyst. 9,
544 Q07015.

545 Masson, D.G, Watts, A.B, Gee, M.J.R, Urgeles, R., Mitchell, N.C., Le Bas, T.P., Canals, M.,
546 2002. Slope failures on the flanks of the western Canary Islands. Earth-Science Reviews 57,
547 1-35.

548 Mitchell, N.C., Masson, D.G., Watts, A.B., Gee, M.J.R., Urgeles, R., 2002. The morphology of
549 the submarine flanks of volcanic ocean islands: A comparative study of the Canary and

Hawaiian hotspot islands. J. Volcanol. Geotherm. Res. 115, 83-107.

Navarro, J.M., Coello, J., 1989. Depressions originated by landslide processes in Tenerife. ESF Meeting on Canarian Volcanism, Lanzarote, pp. 150-152.

Quartau, R., Ramalho. R.S., Madeira, J., Santos, R., Rodrigues, A., Roque, C., Carrara, G, Silveira, A.B., 2018. Gravitational, erosional and depositional processes on volcanic ocean islands: Insights from the submarine morphology of Madeira Archipelago. Earth and Planetary Science Letters 482, 288-299.

Quidelleur, X., Hildenbrand, A., Samper, A., 2008. Causal link between Quaternary paleoclimatic changes and volcanic islands evolution. Geophysical Research Letters 35, 5.

Ramalho, R. S., Helffrich, G., Cosca, M., Vance, D., Hoffmann, D., Schmidt, D. N., 2010. Vertical movements of ocean island volcanoes: Insights from a stationary plate environment. Marine Geology 275, 84-95.

Samrock, L.K., Hansteen, T.H., Dullo, WC., Wartho, J.A., 2022. Internal igneous growth, doming and rapid erosion of a mature ocean island: the Miocene evolution of Maio (Cabo Verde). Int J Earth Sci 111, 1129-1148.

Serralheiro, A. (1976). A Geologia da ilha de Santiago (Cabo Verde). Bol. Museu Lab. Mineral. Geol. Fac. Ciências Lisboa 14.

Sibrant, A., Marques, F. O., Hildenbrand, A., 2014. Construction and destruction of a volcanic island developed inside an oceanic rift: Graciosa Island, Terceira Rift, Azores. Journal of Volcanology and Geothermal Research 284, 32-45.

Sibrant, A.L.R., Hildenbrand, A., Marques, F.O., Costa, A.C.G., 2015a. Volcano-tectonic evolution of the Santa Maria Island (Azores): Implications for paleostress evolution at the

572 western Eurasia–Nubia plate boundary. Journal of Volcanology and Geothermal Research
573 291, 49-62.

574 Sibrant, A. L. R., Hildenbrand, A., Marques, F. O., Weiss, B., Boulesteix, T., Hübscher, C., et
575 al., 2015b. Morpho-structural evolution of a volcanic island developed inside an active
576 oceanic rift: S. Miguel Island (Terceira Rift, Azores). Journal of Volcanology and Geothermal
577 Research 301, 90-106.

578 Stillman, C.J., Furnes, H., Le Bas, M.J., Robertson, A.H.F., Zielonka, J., 1982. The geological
579 history of Maio, Cape Verde Islands. J Geol Soc 139, 347-361.

580 Urgeles, R., Canals, M., Baraza, J., Alonso, B., 1998. Seismostratigraphy of the western flanks
581 of El Hierro and La Palma (Canary Islands): a record of Canary Islands volcanism. Mar. Geol.
582 146, 225-241.

583 Weiß, B., Hübscher, C., Lüdmann, T., Serra, N., 2016. Submarine sedimentation processes in the
584 southeastern Terceira Rift / São Miguel region (Azores). Marine Geology 374, 42-58.

585 Woodhall, D., 1974. Geology and volcanic history of Pico Island Volcano, Azores. Nature 248,
586 663-665.

Figure 01

Click here to access/download;Figure (Color);Fig_01.jpg

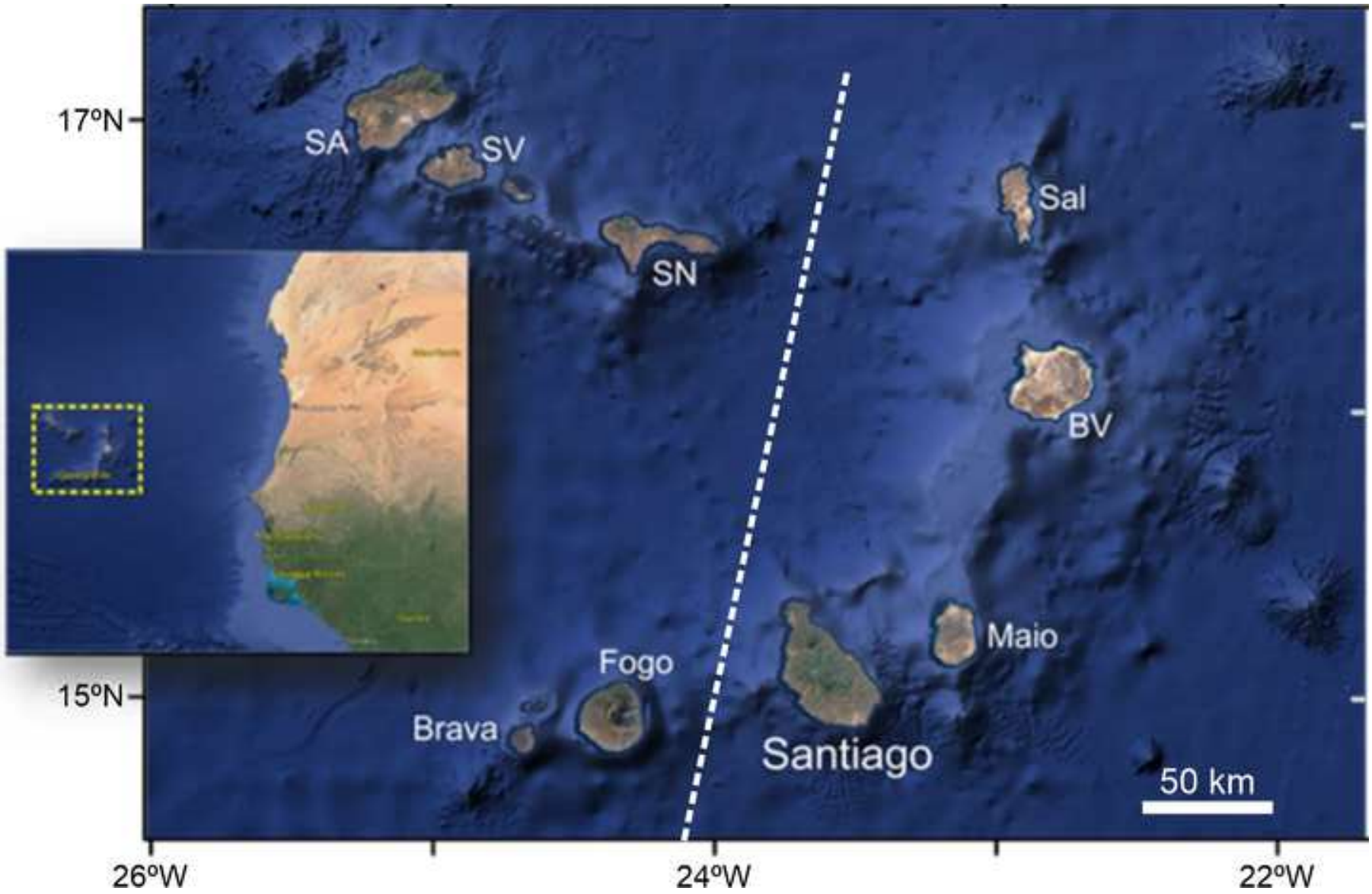

Figure 02

Click here to access/download;Figure (Color);Fig_02.jpg

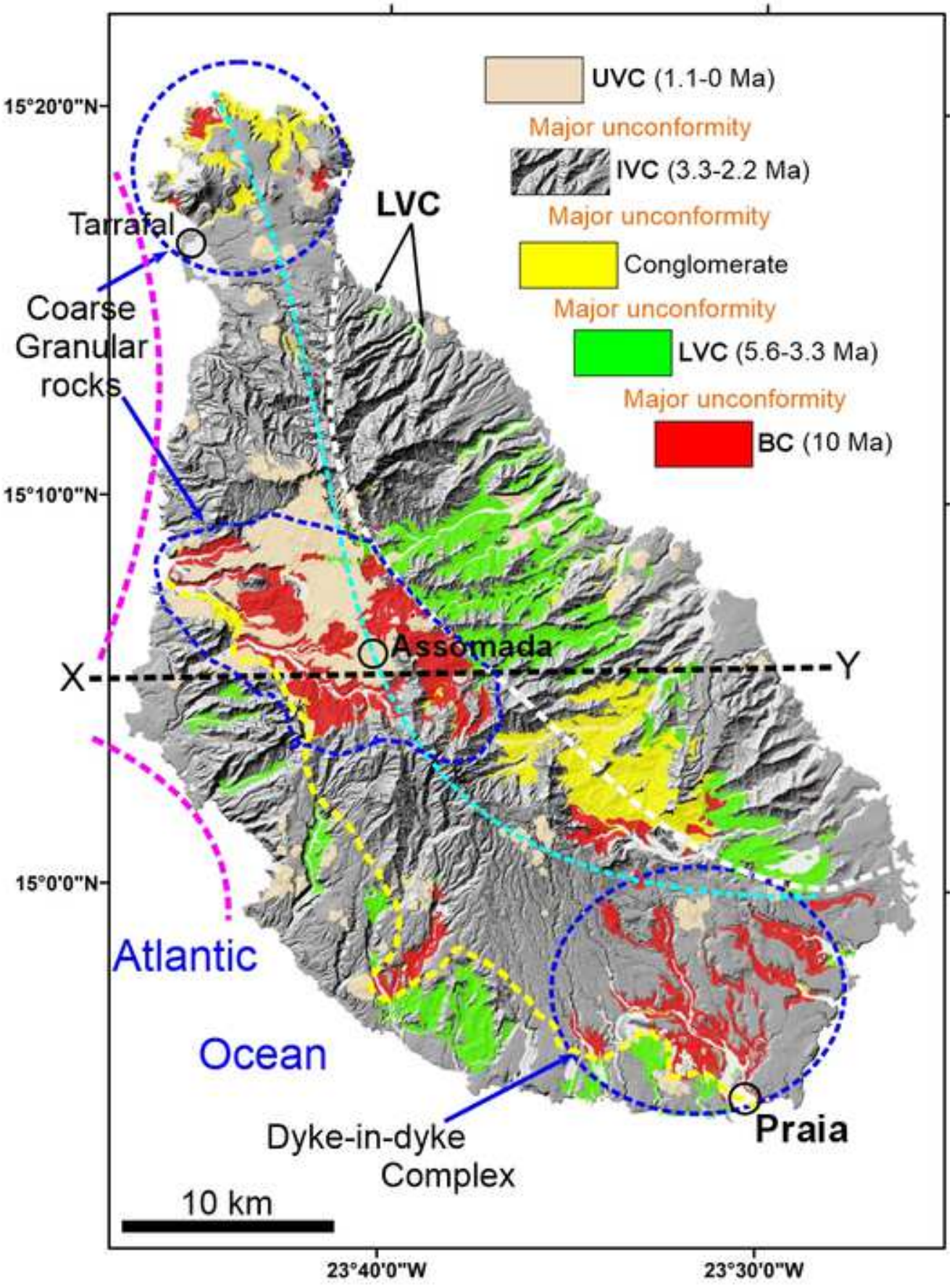

Figure 03

Click here to access/download;Figure (Color);Fig_03.jpg

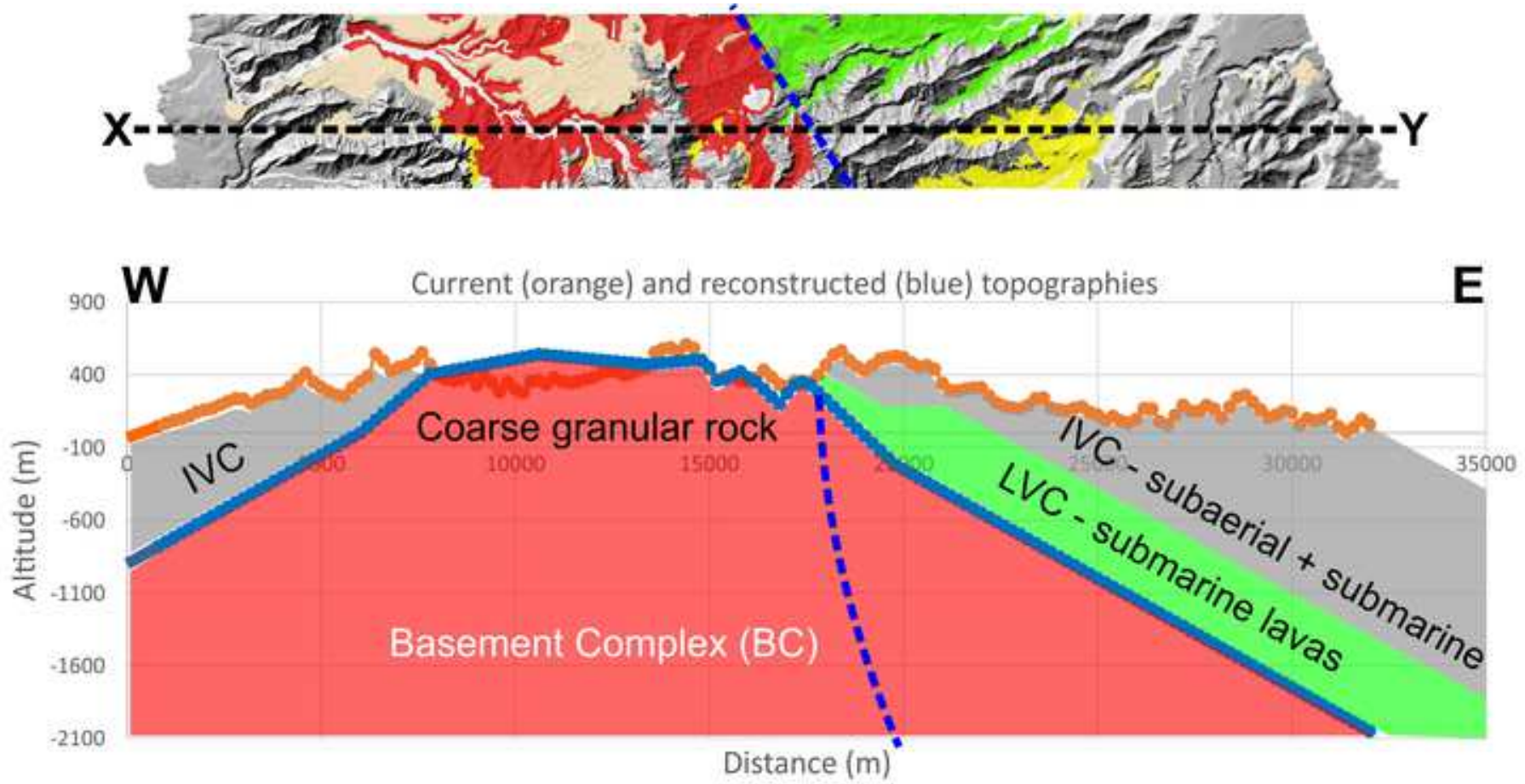

Figure 04

Click here to access/download;Figure (Color);Fig_04.jpg

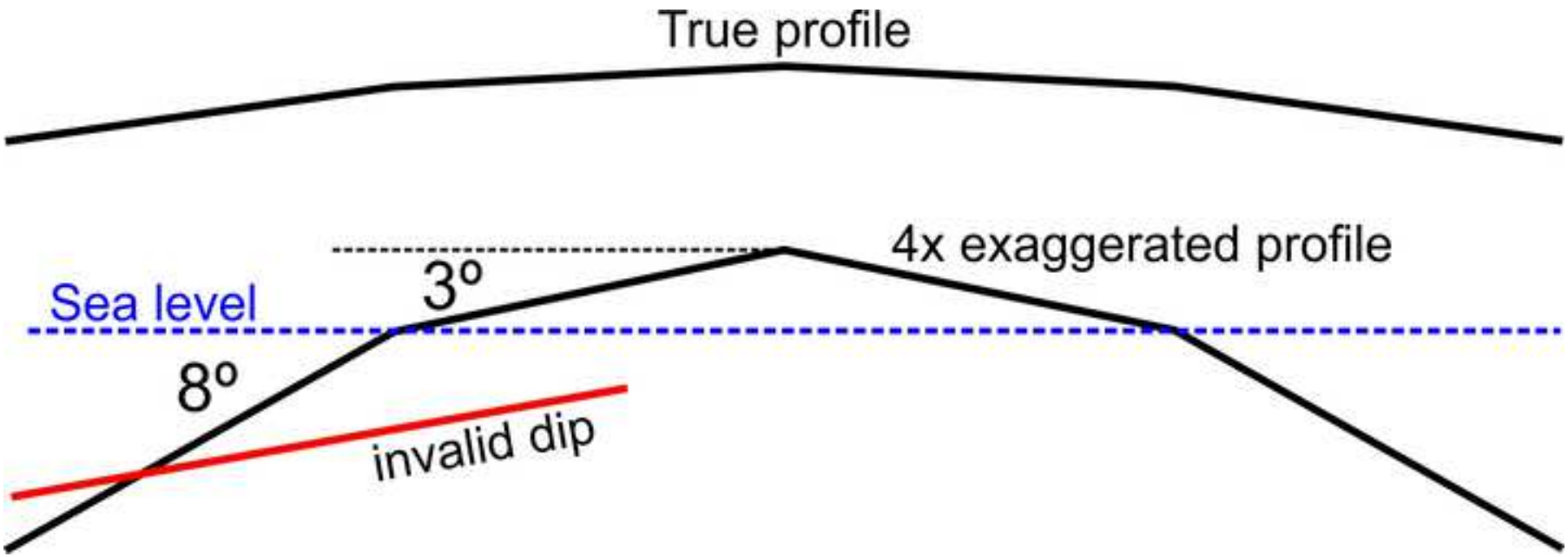

Figure 05

Click here to access/download;Figure (Color);Fig_05.jpg

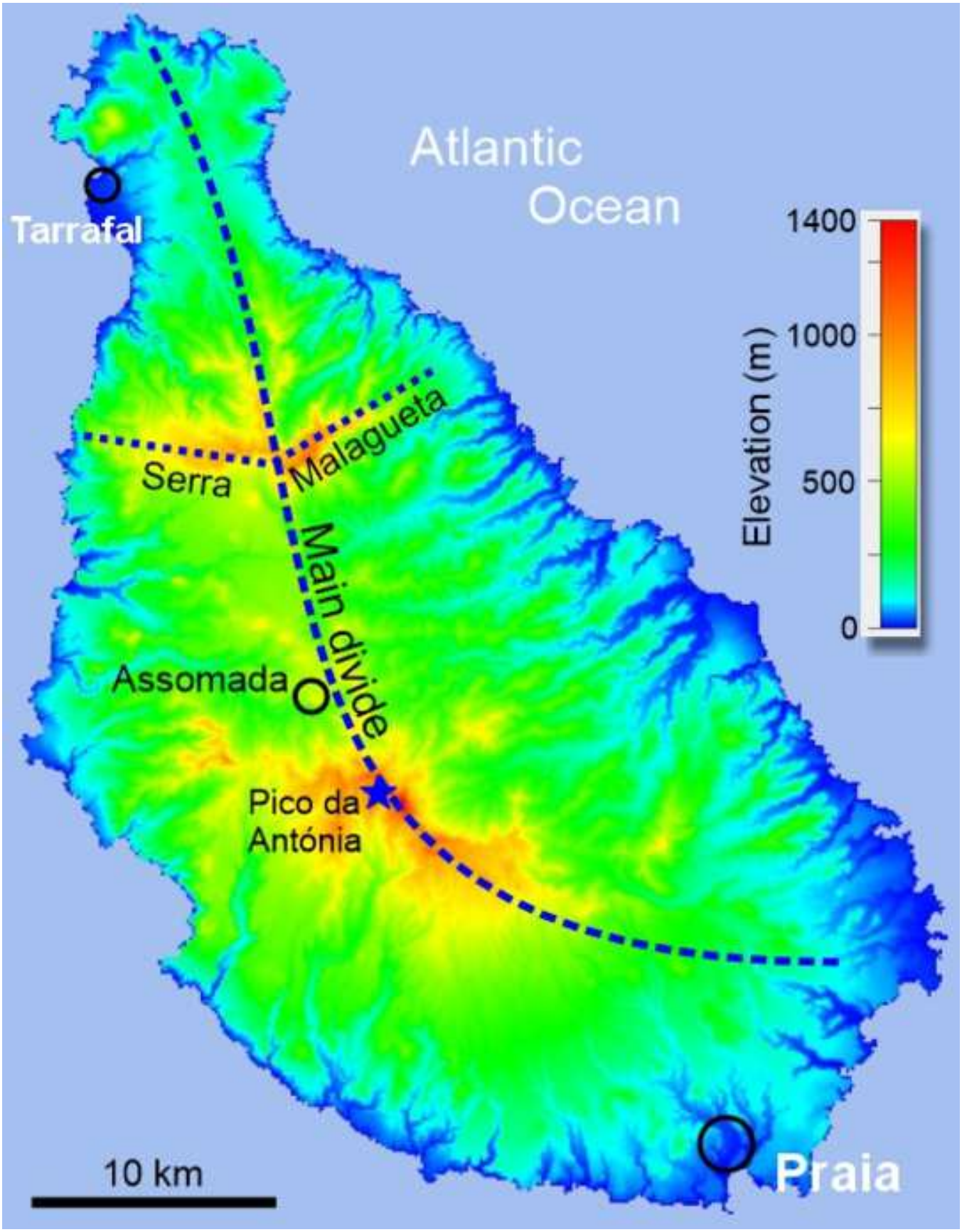

Figure 06

Click here to access/download;Figure (Color);Fig_06_May25.jpg

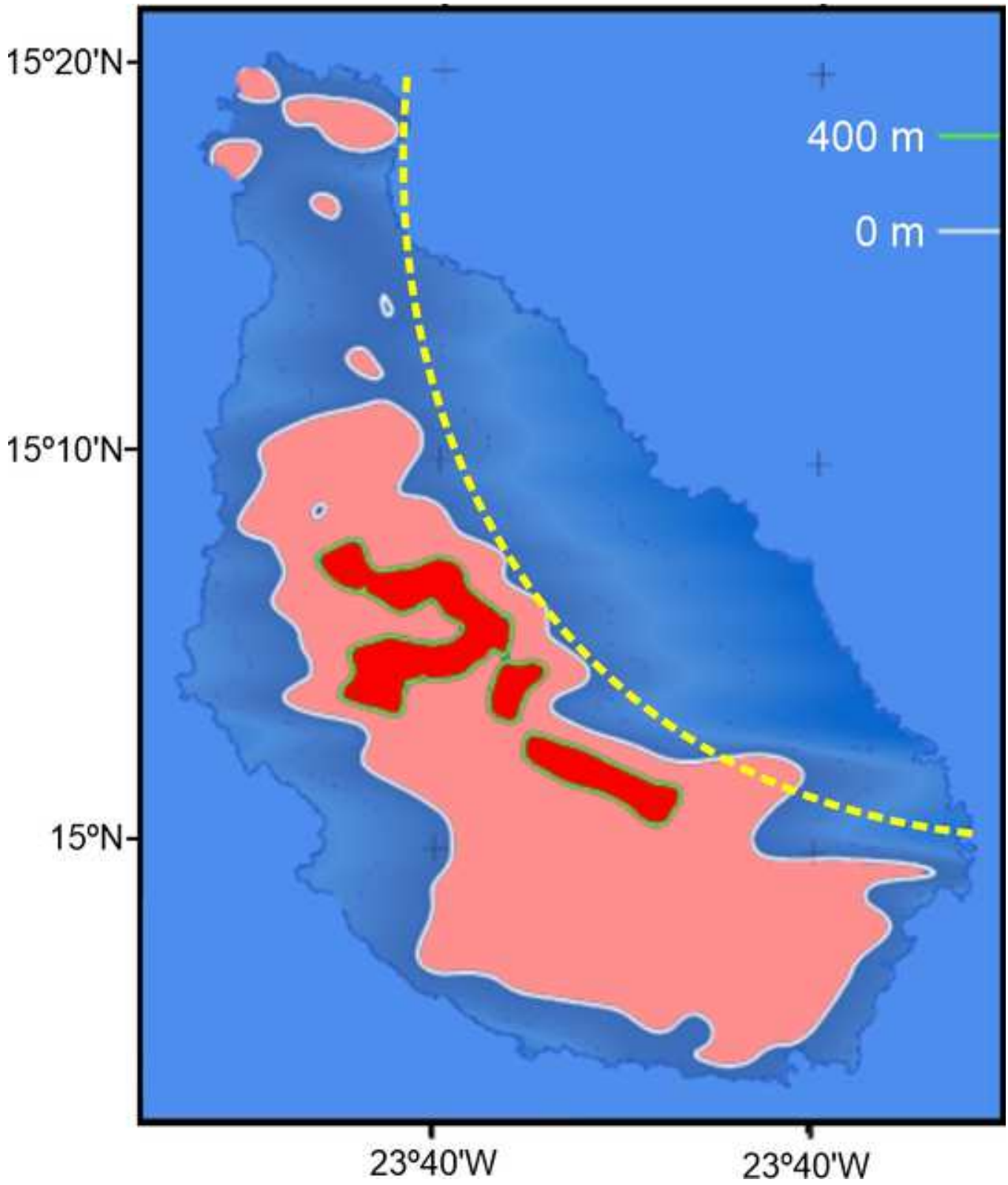

Figure 07

Click here to access/download;Figure (Color);Fig_07.jpg

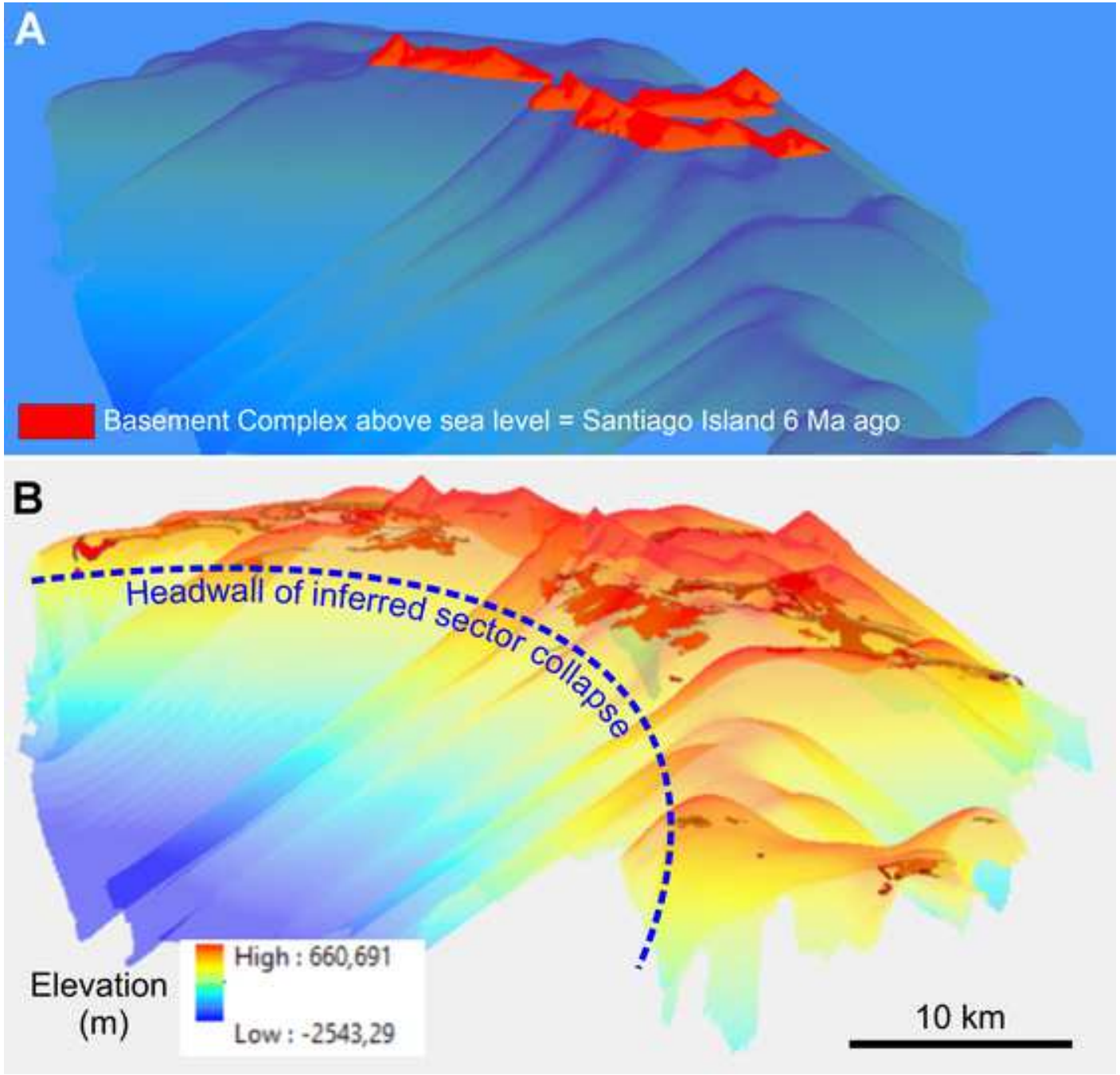

Figure 08

Click here to access/download;Figure (Color);Fig_08.jpg

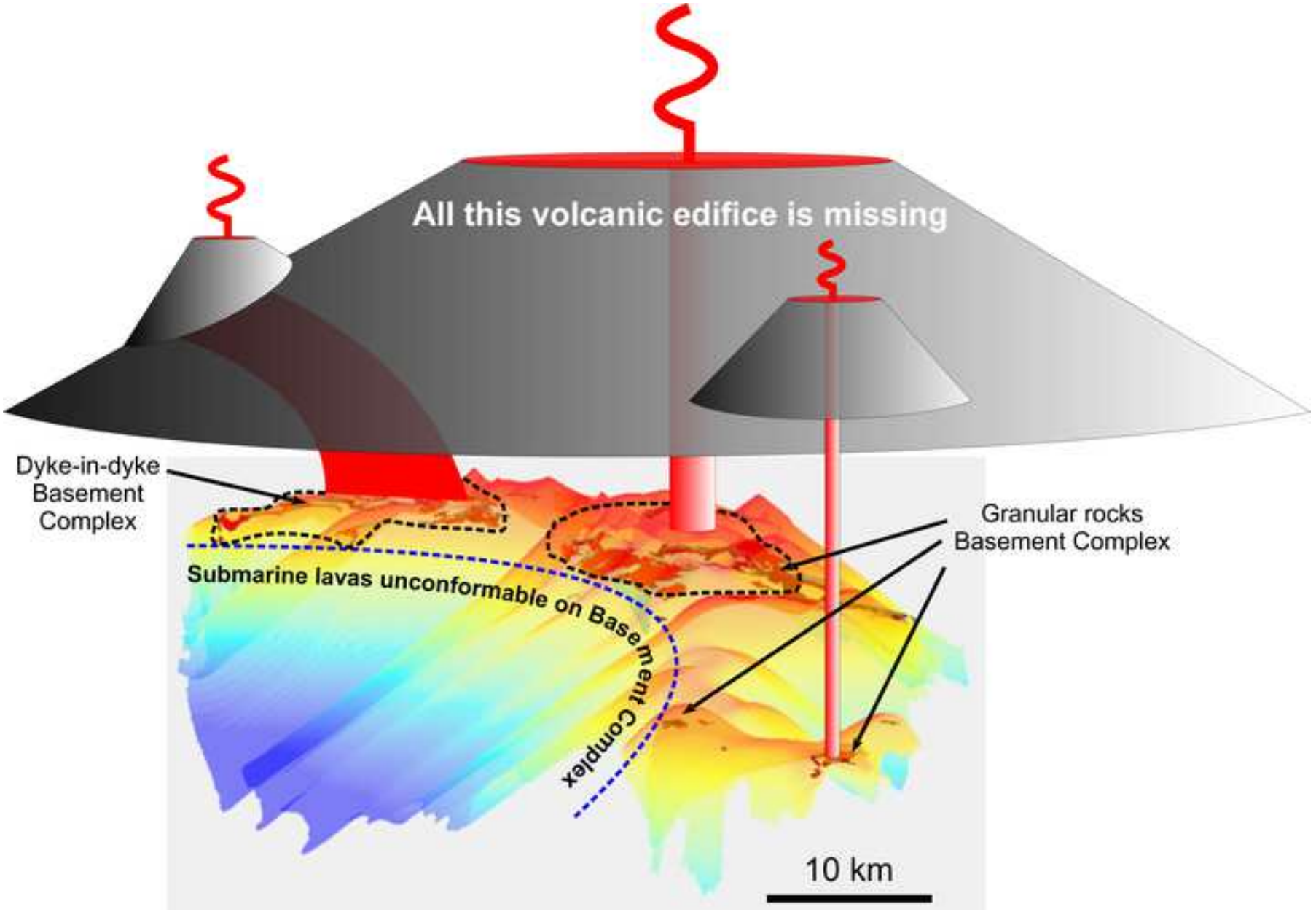

Figure 09

Click here to access/download;Figure (Color);Fig_09.jpg

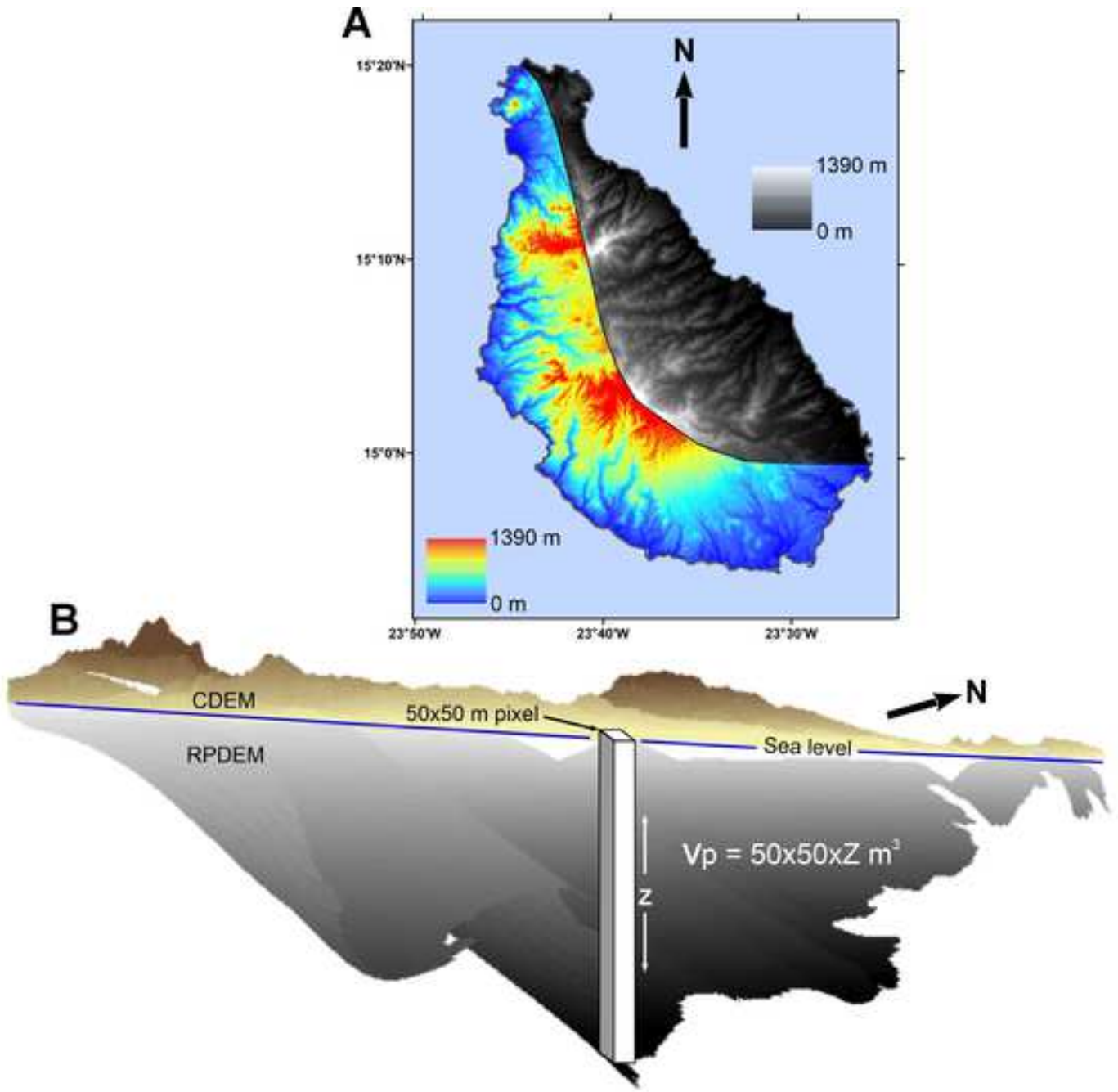

Figure 10

Click here to access/download;Figure (Color);Fig_10.jpg

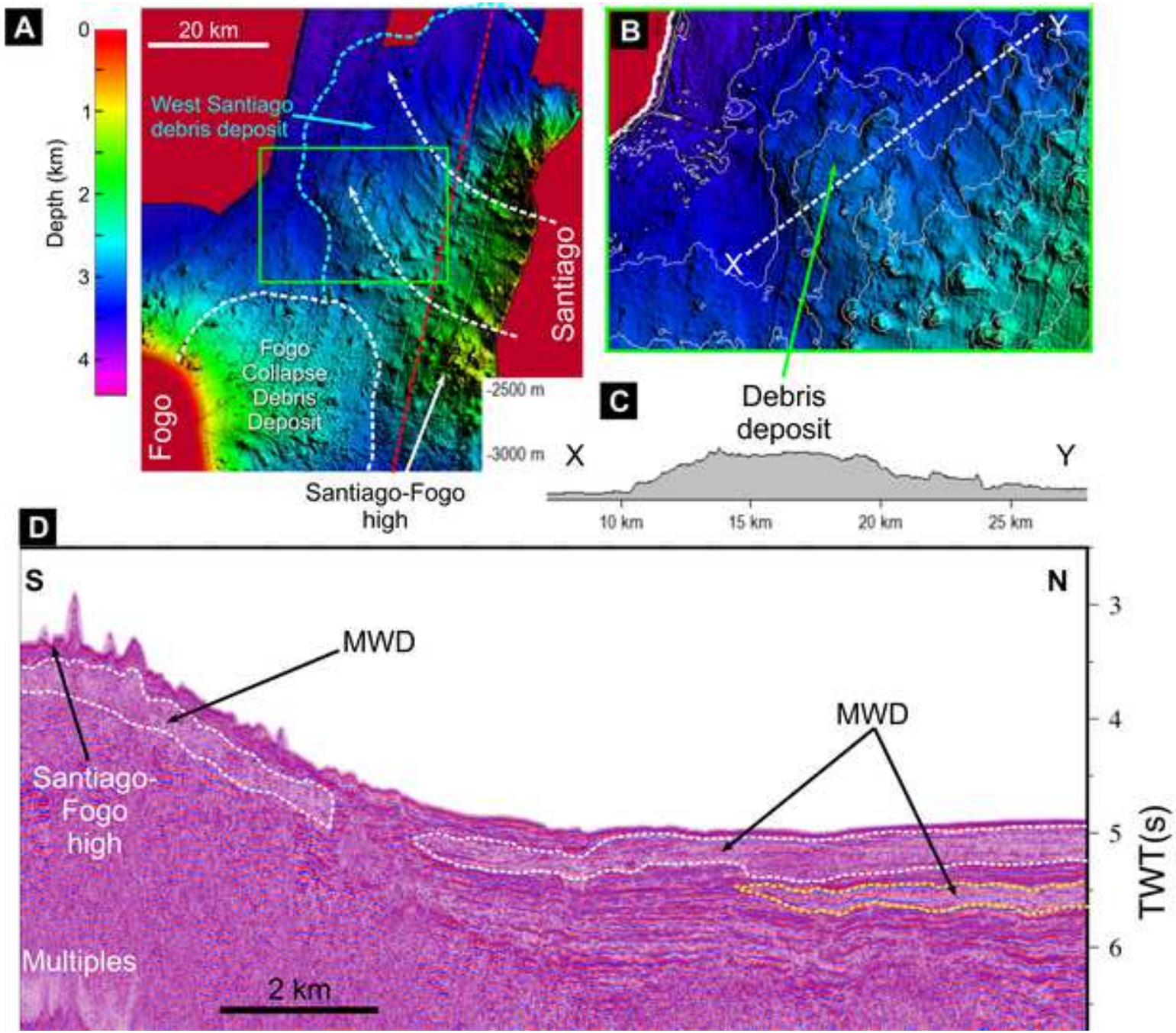

Figure 11

Click here to access/download;Figure (Color);Fig_11.jpg

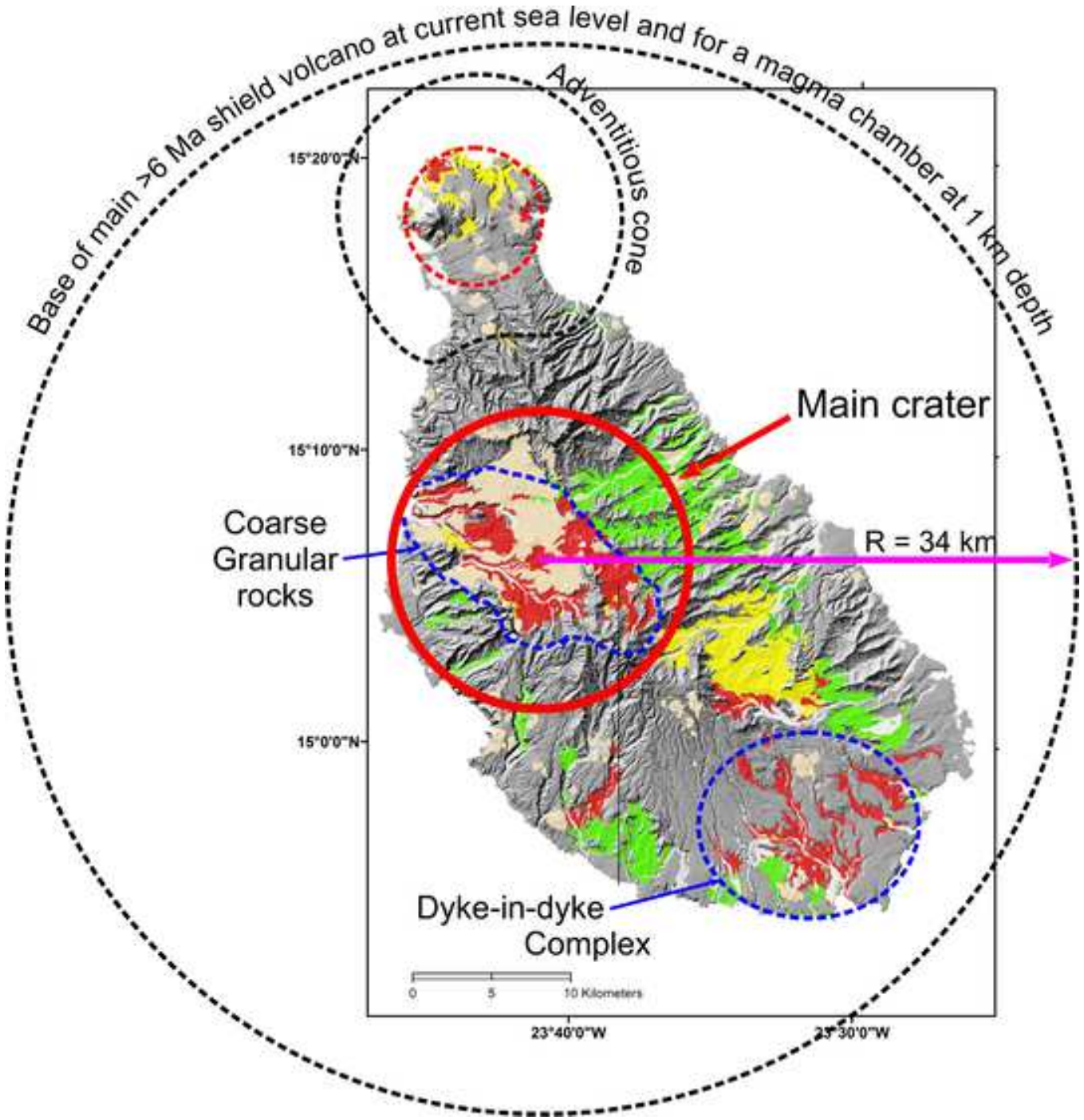

Figure 12

Click here to access/download;Figure (Color);Fig_12.jpg

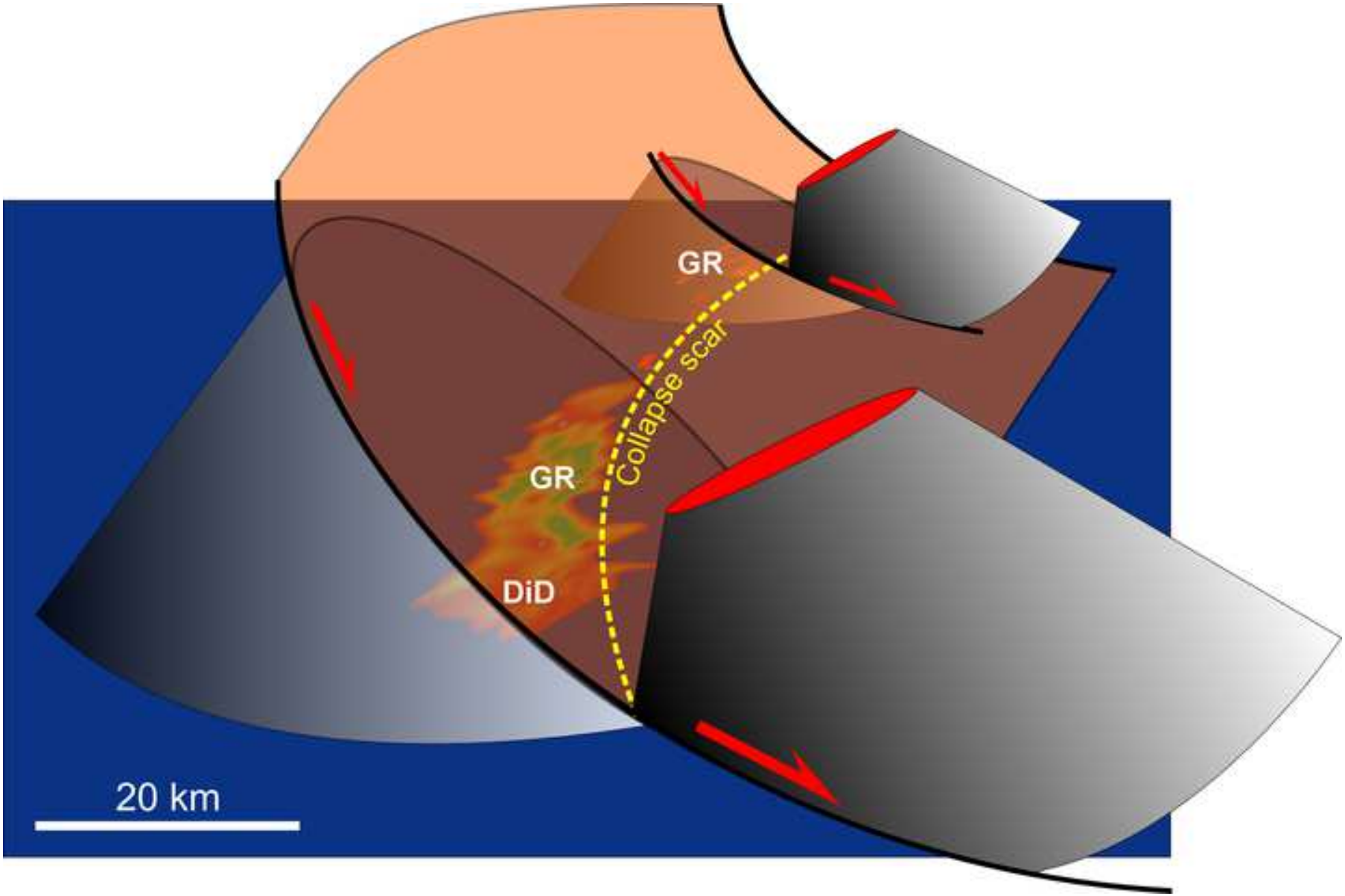

Declaration of Interest Statement

Declaration of interests

☐The authors declare that they have no known competing financial interests or personal relationships that could have appeared to influence the work reported in this paper.

☒The authors declare the following financial interests/personal relationships which may be considered as potential competing interests:

Fernando Ornelas Marques reports a relationship with University of Lisbon Faculty of Sciences that includes: employment.